

Topological data quality via 0-dimensional persistence matchings

Álvaro Torras-Casas^{1,a,*}, Eduardo Paluzo-Hidalgo^{1,b,a}, Rocio Gonzalez-Diaz^{1,a}

^a*University of Sevilla, Campus Reina Mercedes, Sevilla, 41012, Spain*

^b*Quantitative Methods Department, Universidad Loyola Andalucía, Campus Sevilla, Dos Hermanas, Sevilla, 41704, Spain*

Abstract

Data quality is crucial for the successful training, generalization and performance of artificial intelligence models. We propose to measure data quality for supervised learning using topological data analysis techniques. Specifically, we provide a novel topological invariant based on persistence matchings induced by inclusions and using 0-dimensional persistent homology. We show that such an invariant is stable. We provide an algorithm and relate it to images, kernels, and cokernels of the induced morphisms. Also, we show that the invariant allows us to understand whether the subset “represents well” the clusters from the larger dataset or not, and we also use it to estimate bounds for the Hausdorff distance between the subset and the complete dataset. This approach enables us to explain why the chosen dataset will lead to poor performance.

Keywords: Topological feature, computational topology, persistence modules, Vietoris-Rips filtration, triplet merge trees, induced matchings, explainability.

*Corresponding author

Email addresses: `atorras@us.es` (Álvaro Torras-Casas), `epaluzo@uloyola.us.es` (Eduardo Paluzo-Hidalgo), `rogodi@us.es` (Rocio Gonzalez-Diaz)

¹A. Torras-Casas ORCID iD: 0000-0001-9937-0033. E. Paluzo-Hidalgo ORCID iD: 0000-0002-4280-5945. R. Gonzalez-Diaz ORCID iD: 0000-0002-5099-6294.

1. Introduction

Typically, about 80% of the dataset is taken for training while reserving the remaining 20% for testing (or a similar proportion). Often, many training instances are very similar, and the training dataset could be taken in a smaller proportion; i.e. the model is “learning” what it already knows. In addition, large training datasets could bring risks and environmental impacts in some areas, such as natural language processing. See, for example, [2].

As a tool that helps analyze the quality of training datasets, we introduce the new concept of 0-dimensional topological data quality in this paper, which relies on block functions from [8] built on top of persistent homology. This new concept could help, in the future, explain when and why a simple model is enough for a classification task or when a more complex model is necessary.

Our study is done for the case of finite metric spaces X and Z together with an inclusion $X \subseteq Z$. The usual procedure to date computes the persistent homologies $\text{PH}_*(X)$ and $\text{PH}_*(Z)$ obtained from the respective Vietoris-Rips filtration and compares their interval decompositions (also called barcodes), $\text{B}(\text{PH}_*(X))$ and $\text{B}(\text{PH}_*(Z))$, by some distance, such as the bottleneck or Wasserstein distance (see, for example, [3, 7, 4]). However, such comparisons might differ substantially from the underlying distribution of the datasets X and Z , since both distances are based only on combinatorial comparisons between the interval decompositions of $\text{PH}_*(X)$ and $\text{PH}_*(Z)$. Another approach, which we include in our study, is to consider the persistence modules $\text{im}(f)$, $\text{ker}(f)$ and $\text{coker}(f)$ associated with the morphism $f : \text{PH}_*(X) \rightarrow \text{PH}_*(Z)$ induced by the inclusion $X \subseteq Z$. Specifically, we propose an indicator of topological data quality based on the block function \mathcal{M}_f induced by the morphism f , introduced in [8]. Since this paper focuses on 0-dimensional persistent homology, the block function will be denoted as \mathcal{M}_f^0 to highlight this fact. We show that \mathcal{M}_f^0 , $\text{PH}_0(X)$ and $\text{PH}_0(Z)$ encode the same information as $\text{im}(f)$, $\text{ker}(f)$ and $\text{coker}(f)$. However, the advantage of using \mathcal{M}_f^0 is that we can use it to define a single diagram $D(f)$ that combines all the information from $\text{B}(\text{PH}_0(X))$, $\text{B}(\text{PH}_0(Z))$, $\text{B}(\text{im}(f))$, $\text{B}(\text{ker}(f))$ and $\text{B}(\text{coker}(f))$. An additional advantage of using \mathcal{M}_f^0 is that we can compute it using minimum spanning trees, leading to an efficient and simple method that we detail in Section 3. Besides, we show that \mathcal{M}_f^0 is a well-behaved invariant and stable under small perturbations and that redundant information of X and Z are concentrated in $D(f)$ around the origin. Also, we use \mathcal{M}_f^0 to show when a subset “captures well” the connected components of

a given dataset. In addition, we prove that we can use \mathcal{M}_f^0 to obtain the bounds of the Hausdorff distance between X and Z . This further supports the consideration of \mathcal{M}_f^0 as a measure of the topological representativity of a dataset, offering greater flexibility compared to the Hausdorff distance.

We start by reviewing the concept of block functions in Section 2, where we include examples and a novel description of how to compute it in the 0-dimensional case using minimum spanning trees. In Section 3, we provide a pseudocode for the computation of the 0-dimensional induced block function \mathcal{M}_f^0 . Later, in Section 4, we prove the stability of \mathcal{M}_f^0 by using algebraic properties. Afterwards, in Section 5, we study the topological data quality of a subset with respect to the given set and give bounds for the Hausdorff distance between the subset and the given set. Then, Section 6 is devoted to applications of the novel tool previously defined. Section 7 ends the paper with conclusions and future work.

2. Block functions between barcodes induced by finite metric space inclusion maps

Consider a finite metric space Z and a subset X of Z . Since distances are defined between the samples from Z , it is natural to consider the Vietoris-Rips filtration $\text{VR}(X)$ and $\text{VR}(Z)$ to create combinatorial models on the finite metric space. Fixing a ground field, a morphism between the persistent homology of the Vietoris-Rips filtrations can be obtained, and the codification of this information in barcodes and block functions encapsulates rich topological information derived from the inclusion $X \subseteq Z$. Specifically, in this work, we are only interested in the 0-dimensional persistent homology, and so, without loss of generality, we only work with the 1-skeleton of Vietoris-Rips filtrations (that we also denote as VR to unload the notation) and fix \mathbb{Z}_2 as the ground field. Our goal in this section is to explain how to compute a block function from the barcode $B(V)$ to the barcode $B(U)$ induced by the inclusion $X \subseteq Z$, where $U = \text{PH}_0(X)$ and $V = \text{PH}_0(Z)$ are, respectively, the 0-dimensional persistent homologies of $\text{VR}(X)$ and $\text{VR}(Z)$ over \mathbb{Z}_2 .

2.1. Background

First, we need to introduce some technical background from the computational topology field. All the information can be found, for example, in [7, 11].

2.1.1. *Finite metric spaces and the Gromov-Hausdorff distance*

Let M be a finite metric space with metric d^M . Given a pair of subsets $A, B \subseteq M$, we define their pairwise distance as the quantity

$$d^M(A, B) = \min \{d^M(a, b) \text{ for all } a \in A \text{ and } b \in B\}.$$

When considering a pair $A \subseteq M$ and a point $x \in M$, we use the notation $d^M(x, A) = d^M(\{x\}, A)$.

A disadvantage of the definition of distance between subsets is that it is not effective in distinguishing subsets that are potentially very different. If $A \cap B \neq \emptyset$ then $d^M(A, B) = 0$. For this purpose, it is more useful to consider the *Hausdorff* distance

$$d_H^M(A, B) = \max \{ \max \{d^M(a, B) \mid a \in A\}, \max \{d^M(A, b) \mid b \in B\} \},$$

since $d_H^M(A, B) = 0$ if and only if $A = B$.

Given a metric space Z , an isometric embedding of Z into M is denoted by $\gamma_Z : Z \hookrightarrow M$. Now, consider two finite metric spaces, X and X' . To compare X and X' , we might consider isometric embeddings of both objects into metric spaces of M . This leads to the following definition.

Definition 2.1. The *Gromov-Hausdorff* distance between X and X' is

$$d_{GH}(X, X') = \inf_{M, \gamma_X, \gamma_{X'}} \{d_H^M(\gamma_X(X), \gamma_{X'}(X'))\}.$$

Further, consider pairs (X, Z) and (X', Z') where Z and Z' are a couple of metric spaces and where $X \subseteq Z$ and $X' \subseteq Z'$. We define the following Gromov-Hausdorff distance $d_{GH}((X, Z), (X', Z'))$ as the quantity

$$\inf_{M, \gamma_Z, \gamma_{Z'}} \{ \max \{d_H^M(\gamma_Z(X), \gamma_{Z'}(X')), d_H^M(\gamma_Z(Z), \gamma_{Z'}(Z'))\} \}.$$

This distance measures how far two pairs of metric spaces are from being isometric, i.e., from having the same geometric structure. This concept will be used in Subsection 4.3 to prove the stability of the block function \mathcal{M}_f^0 .

2.2. *The 1-skeleton of the Vietoris-Rips filtration, $\text{VR}(Z)$*

Since we are interested in studying the connectivity of a subset with respect to a larger dataset, given a dataset Z with metric d^Z , we consider the 1-skeleton $\text{VR}(Z)$ of the Vietoris-Rips filtration, which is a family of graphs

$$\text{VR}(Z) = \{ \text{VR}_r(Z) \}_{r \in [0, \infty)},$$

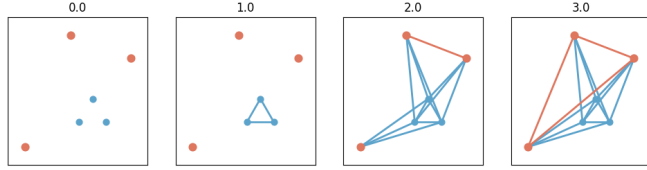


Figure 1: The 1-skeleton of the Vietoris-Rips filtration on X (red) and Z (red and blue).

being r a scale parameter, satisfying that there is an injective morphism of graphs $\text{VR}_r(Z) \hookrightarrow \text{VR}_{r'}(Z)$ for $r \leq r'$. Specifically, fixed $r \geq 0$, $\text{VR}_r(Z)$ is a graph with vertex set Z containing the edge $[x, y]$ with endpoints $x, y \in Z$, whenever the distance between x and y is less than or equal to r , that is, $d^Z(x, y) \leq r$.

Example 2.2. Consider Figure 1. On the left, we depict the set Z consisting of six points, where a sample X is indicated by three red points. As we increase the filtration value, the 1-skeletons of the Vietoris-Rips filtrations increase. We indicate the edges of $\text{VR}_r(X)$ in red and the remaining edges of $\text{VR}_r(Z) \setminus \text{VR}_r(X)$ in blue for values $r \in \{0.0, 1.0, 2.0, 3.0\}$. Notice that, in this particular example, all edges have appeared at the filtration value of 3.0.

2.2.1. Persistence modules

Persistence modules are an algebraic generalization for persistent homology. Specifically, a persistence module V indexed by \mathbb{R} consists of a set of vector spaces $\{V_t\}_{t \in \mathbb{R}}$ and a set of linear maps $\{\rho_{st}^V : V_s \rightarrow V_t\}_{s \leq t}$, called the *structure maps* of V , satisfying that $\rho_{jt}^V \rho_{ij}^V = \rho_{it}^V$ and ρ_{tt}^V being the identity map, for $i \leq j \leq t \in \mathbb{R}$.

Given an interval $I = [a, b) \subset \mathbb{R}$, the *interval module*, κ_I , is a particular case of persistence module consisting of $(\kappa_I)_t = \mathbb{Z}_2$ for all $t \in I$ and $(\kappa_I)_t = 0$ otherwise, while the linear map $\rho_{ij}^{\kappa_I} : (\kappa_I)_i \rightarrow (\kappa_I)_j$ is the identity map whenever $a \leq i \leq j < b$. In this work, for most cases, we consider only interval modules such that $a = 0$. Thus, for ease, we often denote an interval module $\kappa_{[0, b)}$ by the simpler notation κ_b for all $b > 0$. Also, we denote by κ_∞ the persistence module that consists of $(\kappa_\infty)_t = \mathbb{Z}_2$ for all $t \geq 0$ and $(\kappa_\infty)_t = 0$ otherwise; and $\rho_{ij}^{\kappa_\infty} : (\kappa_\infty)_i \rightarrow (\kappa_\infty)_j$ being the identity map whenever $0 \leq i \leq j$ and the zero map otherwise.

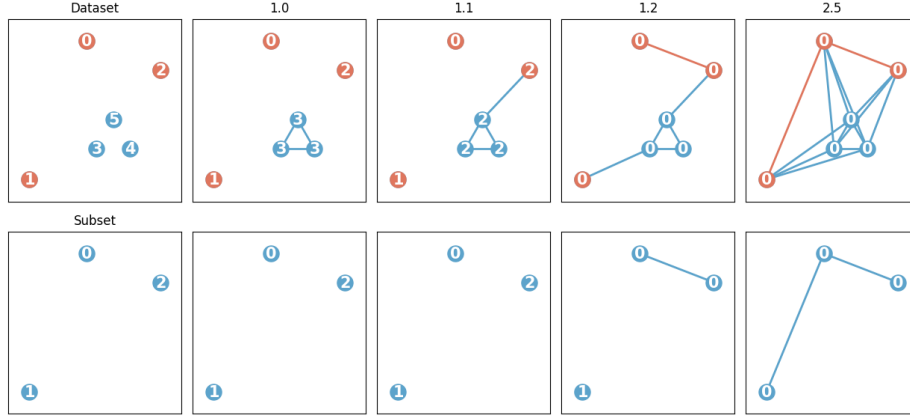


Figure 2: Vietoris-Rips filtration of a set Z (top row) and a subset X (bottom row) with components indexed by non-negative integers.

2.2.2. The 0-dimensional homology group of $\text{VR}_r(Z)$

Fixed $r \geq 0$, the 0-dimensional homology group of $\text{VR}_r(Z)$, is a quotient group, denoted as $H_0(\text{VR}_r(Z))$. Intuitively, it consists of the vector space generated by the classes associated with the connected components of $\text{VR}_r(Z)$.

Specifically, we define $H_0(\text{VR}_r(Z)) = \langle \pi_0(\text{VR}_r(Z)) \rangle$, the free \mathbb{Z}_2 -vector space generated by the set $\pi_0(\text{VR}_r(Z))$ of connected components of $\text{VR}_r(Z)$. To describe $\pi_0(\text{VR}_r(Z))$, suppose that Z has n points, so that $Z = \{z_0, \dots, z_{n-1}\}$. Each $\alpha_r \in \pi_0(\text{VR}_r(Z))$ is associated with a set of points A_r such that:

- 1) for each two points $x, y \in A_r$, there exists a *path* $\{x_0, x_1, \dots, x_\ell\} \subseteq A_r$ satisfying that $x_0 = x$, $x_\ell = y$ and $d^Z(x_{i-1}, x_i) \leq r$ for all $i \in \llbracket \ell \rrbracket$, where the expression $\llbracket \ell \rrbracket$ denotes the set $\{0, 1, \dots, \ell - 1\}$; and
- 2) $d^Z(z, A_r) > r$ for any point $z \in Z \setminus A_r$.

Besides, we denote by $A_r(z)$ the connected component in $\text{VR}_r(Z)$ that contains $z \in Z$. From this viewpoint, $\pi_0(\text{VR}_r(Z)) = Z / \sim$ where \sim is the equivalence relation given by $x \sim y$ if and only if $x \in A_r(y)$. Finally, $\alpha_r \in \pi_0(\text{VR}_r(Z))$ associated with the connected component A_r is always represented by the point of A_r with the lowest label. That is, $\alpha_r = [z_j]$ for some $z_j \in A_r$ such that $j = \min\{\ell \in \llbracket n \rrbracket, | z_\ell \in A_r\}$.

Example 2.3. Consider the same pair $X \subset Z$ from Example 2.2, and suppose that we have labeled the points from X and Z as depicted on the left of Figure 2. Thus, we might write $Z = \{z_0, z_1, z_2, z_3, z_4, z_5\}$ and $X = \{z_0, z_1, z_2\}$. In the same Figure 2, we consider three filtration values ranging over $r \in \{1.0, 1.1, 1.2, 2.5\}$ and we label the vertices of $\text{VR}_r(Z)$ (top row) and $\text{VR}_r(X)$ (bottom row) with the smaller index in their respective connected components. For example, we have $\text{H}_0(\text{VR}_{1.2}(Z)) = \langle [z_0] \rangle$ while $\text{H}_0(\text{VR}_{1.2}(X)) = \langle [z_0], [z_1] \rangle$.

2.2.3. The 0-dimensional persistent homology of $\text{VR}(Z)$ and merge trees

The 0-dimensional persistent homology of $\text{VR}(Z)$, denoted as $U = \text{PH}_0(Z)$, is an algebraic structure that *encapsulates* the 0-dimensional topological events that occur within the filtration. Specifically, U is a *persistence module* given by the set $\{U_r = \text{H}_0(\text{VR}_r(Z))\}_{r \in [0, \infty)}$ of 0-dimensional homology groups and the set of linear maps

$$\{\rho_{rs}^U : \text{H}_0(\text{VR}_r(Z)) \rightarrow \text{H}_0(\text{VR}_s(Z))\}_{r \leq s}$$

that are induced by $\text{VR}_r(Z) \hookrightarrow \text{VR}_s(Z)$. In particular, given $\alpha_r = [z_j] \in \pi_0(\text{VR}_r(Z))$, we have that:

$$\rho_{rs}^U([z_j]) = \begin{cases} [z_j] & \text{if } d^Z(A_s(z_j), A_s(z_\ell)) > s \text{ for all } \ell \in \llbracket j \rrbracket, \\ [z_i] & \text{for some } i \in \llbracket j \rrbracket \text{ such that } A_s(z_j) = A_s(z_i). \end{cases}$$

Thus, if $\rho_{rs}^U([z_j]) = [z_j]$, then we deduce that $A_s(z_j)$ is represented by z_j . On the other hand, if $\rho_{rs}^U([z_j]) = [z_i]$ for some $i \in \llbracket j \rrbracket$, then $A_s(z_j)$ is represented by z_i .

Intuitively, $\text{PH}_0(Z)$ encapsulates the evolution of connected components in $\text{VR}(Z)$. These components start being the isolated points of the whole dataset Z and, as the filtration parameter increases, $\text{PH}_0(Z)$ records the death values of such components. In this way, all classes in $\text{PH}_0(Z)$ are *born* at 0, meaning that $\pi_0(\text{VR}_0(Z)) = \{ [z_i] \mid i \in \llbracket n \rrbracket \}$. On the other hand, a class $[z_j] \in \text{H}_0(\text{VR}_0(Z))$ is said to *die* at $b > 0$ if:

- 1) $d^Z(A_r(z_j), A_r(z_\ell)) > r$ for all $\ell \in \llbracket j \rrbracket$ and $r \in [0, b)$; and
- 2) $A_b(z_j) = A_b(z_i)$ for some $i \in \llbracket j \rrbracket$.

Observe that $A_b(z_j) = A_b(z_i)$, and $\rho_{0b}^U([z_j]) = \rho_{0b}^U([z_i]) = [z_i]$, concluding that the class $\alpha_0 = [z_j] + [z_i] \in \text{H}_0(\text{VR}_0(Z))$ belongs to $\ker \rho_{0b}^U$.

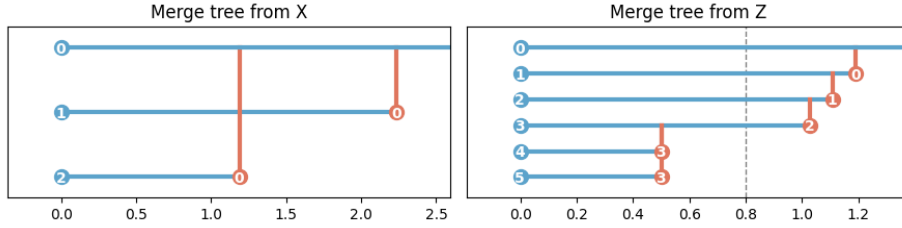


Figure 3: Merge tree representation for X and Z . Triplets (z_j, b_j, z_i) are plotted as a blue horizontal segment labeled by j on the left and i on the right, followed by a red vertical segment that connects to the horizontal segment labeled by i . In addition, on top of the representation, we plot a horizontal blue line corresponding to the component $[z_0]$, which never dies. The blue horizontal intervals compound the barcodes of $\text{PH}_0(X)$ (on the left) and $\text{PH}_0(Z)$ (on the right). Notice that, in both representations, we have sorted the horizontal blue lines by increasing death values.

We consider the set of triplets $(z_j, b_j, z_i) \in Z \times \mathbb{R}_{>0} \times Z$ such that $[z_j] \in H_0(\text{VR}_0(Z))$ dies at value $b_j > 0$ and $\rho_{0b_j}^U([z_j]) = [z_i]$, here we ignore the component $[z_0]$ which never *dies*. We denote such set as $\text{TMT}(Z)$ and call it the *triplet merge tree* of Z ; this represents the *merge tree* of $\text{VR}(Z)$. Notice that this is a variant of the original definition from [12], which we modify for convenience in our case as there is no total order in the edge set, and several edges might appear at the same filtration value. Let us see an example.

Example 2.4. We consider again Example 2.3 and track the connected components from both $\text{VR}(X)$ and $\text{VR}(Z)$. For example, $\text{TMT}(X)$ contains the triplets $(z_2, 1.19, z_0)$ and $(z_1, 2.24, z_0)$. Such triplets are depicted on the left of Figure 3 such that, for example, triplet $(z_2, 1.19, z_0)$ is plotted as a blue horizontal segment labeled by 2 on the left and 0 on the right, followed by a red vertical segment that connects to the horizontal segment of 0. The resulting representation encodes the merge tree information from $\text{VR}(X)$. On the right of Figure 3, we repeat the same principle using Z . An advantage of representing merge trees is that we know instantly $H_0(\text{VR}_r(Z))$ for all $r \geq 0$. For example, choosing $r = 0.8$, we consider the dashed vertical line on the right merge tree representation of Figure 3; such line crosses four blue segments so that $H_0(\text{VR}_r(Z)) = \langle [z_0], [z_1], [z_2], [z_3] \rangle$.

One reason to consider triplet merge trees is that using a minimum spanning tree for $\text{VR}(Z)$, one can obtain $\text{TMT}(Z)$ directly, as we explain briefly in Section 3. Another reason is that they help understand the operators \ker_b^\pm

that will be used in Subsection 2.3. Basically, given the persistence module $U = \text{PH}_0(Z)$ with structure maps ρ^U , the operators \ker_b^\pm are defined as follows, for all $b > 0$,

$$\ker_b^-(U) = \bigcup_{0 \leq r < b} \ker(\rho_{0r}^U) \quad \text{and} \quad \ker_b^+(U) = \ker(\rho_{0b}^U),$$

and encapsulate the classes in $\text{PH}_0(Z)$ that die at r for $r < b$ and $r \leq b$, respectively. We might write these operators by considering subsets of $\text{H}_0(\text{VR}_0(Z))$ that are defined using triplet merge trees as follows

$$\ker_b^-(U) = \langle [z_i] + [z_j] \mid (z_j, b_j, z_i) \in \text{TMT}(Z) \text{ and } b_j < b \rangle$$

and

$$\ker_b^+(U) = \langle [z_i] + [z_j] \mid (z_j, b_j, z_i) \in \text{TMT}(Z) \text{ and } b_j \leq b \rangle.$$

Example 2.5. Consider $V = \text{PH}_0(X)$ from Example 2.4 and recall that $\text{TMT}(X)$ consists of triplets $(z_2, 1.19, z_0)$ and $(z_1, 2.24, z_0)$; this is depicted on the left of Figure 3. Then we have:

$$\ker_{2.24}^-(V) = \langle [z_2] + [z_0] \rangle \quad \text{and} \quad \ker_{2.24}^+(V) = \langle [z_2] + [z_0], [z_1] + [z_0] \rangle.$$

2.2.4. Barcodes, persistence diagrams, multisets and partial matchings

It is known that, in general, a persistence module V has a unique decomposition as a direct sum of interval modules (see [6]). The interval modules are in bijection with intervals over \mathbb{R} , so V is uniquely characterized by a *multiset* called barcode.

Recall that a multiset is a pair (S, m) composed of a set S together with an assignment $m : S \rightarrow \mathbb{Z}_{\geq 0} \cup \{\infty\}$ that maps elements from S to their multiplicity. The representation of a multiset (S, m) is the set

$$\text{Rep}(S, m) = \{ (s, \ell) \mid s \in S \text{ and } \ell \in \llbracket m(s) \rrbracket \}.$$

Notice that the persistence modules we will deal with in this paper are uniquely characterized by multisets of intervals that involve finite sets and finite multiplicities. Besides, given a persistence module U that consists of the 0-dimensional persistent homology of the Vietoris-Rips filtration of a finite metric space Z , there is a multiset $\text{B}(U) = (S^U, m^U)$, where S^U is a set of intervals from \mathbb{R} together with an assignment called *multiplicity*, $m^U : S^U \rightarrow \mathbb{Z}_{\geq 0}$, satisfying that there is an isomorphism

$$U \simeq \left(\bigoplus_{(J,\ell) \in \text{Rep B}(U)} \kappa_J \right) \oplus \kappa_\infty = \left(\bigoplus_{J \in S^U} \bigoplus_{\ell \in \llbracket m^U(J) \rrbracket} \kappa_J \right) \oplus \kappa_\infty.$$

Specifically, its barcode, $\text{B}(U) = (S^U, m^U)$, is such that all intervals from S^U are of the form $[0, b)$ for values $b > 0$. This is why we might consider S^U as a subset of \mathbb{R} , where an interval $[0, b)$ is substituted by its endpoint b . Notice that, in this paper, we do not consider the infinity interval $[0, \infty)$ as an element from $\text{B}(U)$. Similarly, we also write $m^U(b)$ and κ_b instead of $m^U(J)$ and κ_J without ambiguities. Besides, since Z is finite, we have that $m^U(b) < \infty$. Then,

$$U \simeq \left(\bigoplus_{b>0} \bigoplus_{\ell \in \llbracket m^U(b) \rrbracket} \kappa_b \right) \oplus \kappa_\infty.$$

These intervals track when connected components merge. In particular, there is a bijection between $\text{Rep B}(U)$ and $Z \setminus \{z_0\}$ in the sense that, for each $b > 0$ and $\ell \in \llbracket m^U(b) \rrbracket$, the pair $([0, b), \ell)$ can be univocally associated with a class $[z_j] \in \text{PH}_0(Z)$ that dies at b .

Remark 2.6. There is an isomorphism $\text{TMT}(Z) \simeq \text{Rep B}(U)$ given by sending a triplet $(z_j, b_j, z_i) \in \text{TMT}(Z)$ to $([0, b_j), k) \in \text{Rep B}(U)$ for some $k \in \llbracket m^U(b_j) \rrbracket$.

Example 2.7. Here we consider $U = \text{PH}_0(Z)$ from Example 2.4 again. In this case, $\text{TMT}(Z)$ is composed of $(z_5, 0.50, z_3)$, $(z_4, 0.50, z_3)$, $(z_3, 1.03, z_2)$, $(z_2, 1.11, z_1)$ and $(z_1, 1.19, z_0)$. In other words, both $[z_5], [z_4] \in U_0$ die at value 0.50, $[z_3] \in U_0$ dies at value 1.03, $[z_2] \in U_0$ dies at value 1.11 and $[z_1] \in U_0$ dies at value 1.19; while the class $[z_0] \in U_0$ never dies. Thus,

$$U \simeq \kappa_{0.50} \oplus \kappa_{0.50} \oplus \kappa_{1.03} \oplus \kappa_{1.11} \oplus \kappa_{1.19} \oplus \kappa_\infty.$$

That is $\text{B}(U) = (S^U, m^U)$ with $S^U = \{0.50, 1.03, 1.11, 1.19\}$ and also $m^U(0.50) = 2$ and $m^U(1.03) = m^U(1.11) = m^U(1.19) = 1$. A representation of the barcode $\text{B}(U)$ is plotted by the finite horizontal blue segments on the right in Figure 3.

Another representation of barcodes is the *persistence diagrams*, consisting of a set of points (p, q) in the cartesian plane representing a homology class born at p and dies at q . In Subsection 4.2, we present a diagram representation for \mathcal{M}_f^0 similar to persistence diagrams and study its key differences.

2.2.5. Bottleneck distance and stability of $\text{PH}_0(X)$

Given a pair of multisets (S, m) and (S', m') , a partial matching

$$\sigma : \text{Rep}(S, m) \rightarrow \text{Rep}(S', m')$$

is a bijection $T \rightarrow T'$ for two subsets $T \subseteq \text{Rep}(S, m)$ and $T' \subseteq \text{Rep}(S', m')$. For ease, we use the notation $\text{coim}(\sigma) = T$ and $\text{im}(\sigma) = T'$.

Now, consider two barcodes $B(V)$ and $B(V')$ for two persistence modules V and V' . A ε -matching between $B(V)$ and $B(V')$ is a partial matching $\sigma^V : \text{Rep} B(V) \rightarrow \text{Rep} B(V')$ such that:

- 1) all $([a, b], i) \in \text{Rep} B(V) \setminus \text{coim}(\sigma^V)$ are such that $|b - a| < \varepsilon$,
- 2) all $([a, b], i) \in \text{coim}(\sigma^V)$ are such that $\sigma^V([a, b], i) = ([a', b'], j)$ with $|a - a'| < \varepsilon$ and $|b - b'| < \varepsilon$
- 3) all $([a', b'], j) \in B(V') \setminus \text{im}(\sigma^V)$ are such that $|a' - b'| < \varepsilon$.

This leads us the definition of the *bottleneck distance* between $B(V)$ and $B(V')$, given by

$$d_B(B(V), B(V')) = \inf \{ \varepsilon \mid \exists \varepsilon\text{-matching between } B(V) \text{ and } B(V') \}.$$

The following well-known result will be used in the following subsection.

Proposition 2.8. *Let X and X' be two finite metric spaces. Let $V = \text{PH}_0(V)$ and $V' = \text{PH}_0(X')$. Then, $d_B(B(V), B(V')) \leq 2d_{GH}(X, X')$.*

PROOF. The statement is a consequence of combining Proposition Appendix A.1 with Proposition Appendix A.2. \square

2.2.6. Persistence morphisms

A *persistence morphism* $f : V \rightarrow U$ between persistence modules V and U is a set of linear maps $\{f_t : V_t \rightarrow U_t\}_{t \in \mathbb{R}}$ that commute with the structure maps ρ^V of V and ρ^U of U . That is, $\rho_{st}^U f_s = f_t \rho_{st}^V$ for all $s \leq t$ in \mathbb{R} .

Now, consider a persistence morphism $f : V \rightarrow U$ between $V = \text{PH}_0(X)$ and $U = \text{PH}_0(Z)$ (we do not need to assume now that $X \subseteq Z$). Since all intervals of the barcodes $B(V)$ and $B(U)$ starting at 0, then there are no nested intervals, so we might adapt Theorem 5.3 from [9] as follows.

Then, there are bounds to the bottleneck distances:

$$\begin{aligned} d_B(\mathbf{B}(\ker(f)), \mathbf{B}(\ker(f'))) &\leq 2\varepsilon, \\ d_B(\mathbf{B}(\operatorname{im}(f)), \mathbf{B}(\operatorname{im}(f'))) &\leq 2\varepsilon, \\ d_B(\mathbf{B}(\operatorname{coker}(f)), \mathbf{B}(\operatorname{coker}(f'))) &\leq 2\varepsilon. \end{aligned}$$

2.3. *From inclusion maps to block functions: the induced block function \mathcal{M}_f^0*

The theoretical results supporting the process explained in this section can be consulted in [8]. There, the authors defined a block function $\mathcal{M}_f : S^V \times S^U \rightarrow \mathbb{Z}_{\geq 0}$ induced by a persistence morphism $f : V \rightarrow U$ and provided a matrix-reduction algorithm to compute it. In this subsection, we adapt the construction of \mathcal{M}_f to our particular case of interest.

In our present case, the definition of the block function is simplified as follows. Let $f : V \rightarrow U$ be a persistence morphism between $V = \operatorname{PH}_0(X)$ and $U = \operatorname{PH}_0(Z)$ (we do not need to assume now that $X \subseteq Z$). For $I = [0, a]$ and $J = [0, b]$ we have

$$\mathcal{M}_f^0(I, J) = \dim \left(\frac{f(\ker_a^+(V)) \cap \ker_b^+(U)}{f(\ker_a^-(V)) \cap \ker_b^+(U) + f(\ker_a^+(V)) \cap \ker_b^-(U)} \right).$$

Given $a, b > 0$, we write $\mathcal{M}_f^0(a, b)$ instead of $\mathcal{M}_f^0([0, a], [0, b])$ to simplify notation. This definition has a direct interpretation in terms of barcodes of $\operatorname{im}(f)$, $\ker(f)$ and $\operatorname{coker}(f)$, which we will study in Section 4. In particular, $\mathcal{M}_f^0(a, b) = 0$ for values $a > b$.

The following result states that \mathcal{M}_f^0 always induces a unique partial matching denoted by σ^f .

Lemma 2.11. *Given a persistence morphism $f : V \rightarrow U$, where $V = \operatorname{PH}_0(X)$ and $U = \operatorname{PH}_0(Z)$, the block function \mathcal{M}_f^0 induces a unique partial matching $\sigma^f : \operatorname{Rep} \mathbf{B}(V) \rightarrow \operatorname{Rep} \mathbf{B}(U)$.*

PROOF. To start, recall Theorem 4.4 from [8] which states that \mathcal{M}_f is well-defined, and Theorem 5.1 from [8] which states that \mathcal{M}_f is linear with respect to the direct sums of morphisms. Consequently, the block function \mathcal{M}_f^0 is well-defined and linear with respect to the direct sums of morphisms. In particular, for any $I = [0, a] \in S^V$ with multiplicity $m^V(a)$, \mathcal{M}_f^0 is such that

$$\sum_{b \leq a} \mathcal{M}_f^0(a, b) \leq m^V(a). \quad (1)$$

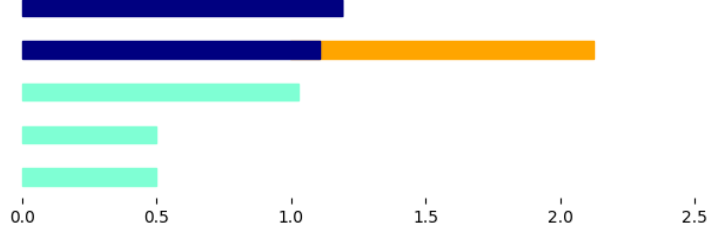


Figure 4: Depiction of the partial matching induced by the block function \mathcal{M}_f^0 from Example 2.12 where we follow the convention: 1) plot horizontal intervals $[0, b)$ for $([0, b), j) \in \text{Rep B}(U)$ by increasing endpoints; 2) if $([0, b), j) \in \text{im}(\sigma^f)$ we plot the interval $[0, b)$ in dark blue, while otherwise, if $([0, b), j) \notin \text{im}(\sigma^f)$, we plot it in light blue; 3) for $([0, a), i) \in \text{Rep B}(V)$ and if $\sigma^f([0, a), i) = ([0, b), j)$ then we plot the interval $[b, a)$ in orange, following the corresponding interval $[0, b)$ for $([0, b), j)$.

Besides, Theorem 5.5 from [8] states that if there are no nested intervals, then $\sum \mathcal{M}_f(I, J) \leq m^U(J)$. Now, since all intervals start at 0, for any interval $J = [0, b) \in S^U$ with multiplicity $m^U(b)$, we have that

$$\sum_{a>b} \mathcal{M}_f^0(a, b) \leq m^U(b). \quad (2)$$

Altogether, by inequalities (1) and (2), it follows that \mathcal{M}_f^0 induces a unique partial matching $\sigma^f : \text{Rep B}(V) \dashrightarrow \text{Rep B}(U)$. \square

Later, in Section 4, we will see that inequality (1) is, in fact, equality, so that σ^f is, in fact, an injection.

Example 2.12. We consider $X \subseteq Z$ from Example 2.3 and recall the computation of $\text{B}(U)$ from Example 2.7, that is, $\text{B}(U) = (S^U, m^U)$ with $S^U = \{0.50, 1.03, 1.11, 1.19\}$ and $m^U(1.03) = m^U(1.11) = m^U(1.19) = 1$ and $m^U(0.50) = 2$. Also, from Example 2.4, we can observe that $\text{B}(V) = (S^V, m^V)$ is such that $S^V = \{1.19, 2.24\}$ with multiplicities $m^V(1.19) = m^V(2.24) = 1$. In Example 3.1, we show, via a matrix procedure, that the matching \mathcal{M}_f^0 is nonzero only for $\mathcal{M}_f^0(1.19, 1.19) = 1$ and $\mathcal{M}_f^0(2.24, 1.11) = 1$. In addition, recalling that $m^U(1.19) = m^U(1.11) = 1$, we see that equations (1) and (2) hold. Then, \mathcal{M}_f^0 induces the partial matching $\sigma^f : \text{Rep B}(V) \dashrightarrow \text{Rep B}(U)$ given by an assignment $([0, 1.19), 0) \mapsto ([0, 1.19), 0)$ and $([0, 2.24), 0) \mapsto ([0, 1.11), 0)$. The resulting barcode, plotted in Figure 4, allows us to instantly visualize which intervals from $\text{Rep B}(U)$ are matched or not and how much the matched intervals differ.

Finally, we state an important property of the induced block function \mathcal{M}_f^0 that follows by Proposition 5.3 from [8].

Proposition 2.13. *Given $b \leq a$, $\mathcal{M}_{\kappa_a \rightarrow \kappa_b}^0(a, b) = 1$ and $\mathcal{M}_{\kappa_a \rightarrow \kappa_b}^0(a', b') = 0$ if either $a' \neq a$ or $b' \neq b$.*

3. A matrix computation procedure for \mathcal{M}_f^0

In this section, we adapt the matrix procedure explained in [8] to calculate the induced block function $\mathcal{M}_f^0 : S^V \times S^U \rightarrow \mathbb{Z}_{\geq 0}$ previously defined.

3.1. Computational procedure overview

Below, we provide an overview of the procedure to compute \mathcal{M}_f^0 . First, given finite metric spaces $X \subseteq Z$, we assume that Z has n elements so that $X = \{z_0, \dots, z_{\ell-1}\}$ and $Z = \{z_0, \dots, z_{n-1}\}$ for some $\ell \leq n$. We compute the persistence modules $V = \text{PH}(X)$ and $U = \text{PH}(Z)$, and the barcodes $\text{B}(V)$ and $\text{B}(U)$, using the minimum spanning trees of $\text{VR}(X)$ and $\text{VR}(Z)$ and the triplet merge trees obtained from them, $\text{TMT}(X)$ and $\text{TMT}(Z)$. In particular, we have that $V_0 = \langle [z_0], \dots, [z_{\ell-1}] \rangle$ and $U_0 = \langle [z_0], \dots, [z_{n-1}] \rangle$.

Next, we consider an order in $\text{TMT}(X)$ where $(z_j, b_j, z_i) < (z_k, b_k, z_r)$ if and only if either $b_j < b_k$ or $(b_j = b_k$ and $z_j < z_k)$ and fix the same order in $\text{TMT}(Z)$. We consider the subspaces

$$U_{[0,b)} = \langle [z_i] + [z_j] \mid (z_j, b_j, z_i) \in \text{TMT}(Z) \text{ and } b_j = b \rangle$$

for all $b > 0$ and notice that

$$U_{[0,b)} \simeq \ker_b^+(U) / \ker_b^-(U) \simeq \bigoplus_{r \in \llbracket m^U(b) \rrbracket} \kappa_b.$$

Also, we define $U_{[0,\infty)} = \langle [z_0] \rangle$. In addition, since $\text{Rep B}(U) \simeq \text{TMT}(Z)$, we obtain an isomorphism

$$\beta : \left(\bigoplus_{(z_j, b, z_i) \in \text{TMT}(Z)} \kappa_b \right) \oplus \kappa_\infty \rightarrow U,$$

defined for each component $(z_j, b, z_i) \in \text{TMT}(Z)$, by the morphism $\kappa_b \rightarrow U$ that sends $1 \in (\kappa_b)_0$ to $[z_j] + [z_i] \in U_0$ together with $\kappa_\infty \rightarrow U$ sending $1 \in (\kappa_\infty)_0$ to $[z_0]$. Analogously, we consider the isomorphism

$$\alpha : \left(\bigoplus_{(z_k, a, z_r) \in \text{TMT}(X)} \kappa_a \right) \oplus \kappa_\infty \rightarrow V.$$

Thus, we can consider the composition

$$\beta^{-1}f\alpha : \left(\bigoplus_{(z_k, a, z_r) \in \text{TMT}(X)} \kappa_a \rightarrow \bigoplus_{(z_j, b, z_i) \in \text{TMT}(Z)} \kappa_b \right) \oplus \left(\kappa_\infty \rightarrow \kappa_\infty \right).$$

We pay attention to the matrix F associated with the persistence morphism $\beta^{-1}f\alpha$ ignoring the component $(\kappa_\infty)_0 \rightarrow (\kappa_\infty)_0$. Since by Remark 2.6, we have that $\text{TMT}(X) \simeq \text{Rep B}(V)$ and $\text{TMT}(Z) \simeq \text{Rep B}(U)$ then F is a $\# \text{Rep B}(V) \times \# \text{Rep B}(U)$ matrix with columns indexed by $\text{TMT}(X) \simeq \text{Rep B}(V)$ and rows indexed by $\text{TMT}(Z) \simeq \text{Rep B}(U)$ and with coefficients in \mathbb{Z}_2 . We call F the *associated matrix* to f .

Finally, we compute R , the Gaussian reduction of F , obtained by left-to-right column additions. This leads to a computation for $\mathcal{M}_f^0(a, b)$, for $a \geq 0$ and $b \geq 0$, as

$$\mathcal{M}_f^0(a, b) = \# \left\{ \begin{array}{l} \text{pivots from } R \text{ in columns associated to } ([0, a), t) \\ \text{and rows associated to } ([0, b), r) \\ \text{for all } t \in \llbracket m^V(a) \rrbracket \text{ and } r \in \llbracket m^U(b) \rrbracket \end{array} \right\}.$$

Summing up, we compute \mathcal{M}_f^0 with the following operations:

1. Compute the minimum spanning trees $\text{MST}(X)$ and $\text{MST}(Z)$ of $\text{VR}(X)$ and $\text{VR}(Z)$ respectively.
2. Compute the triplet merge trees $\text{TMT}(X)$ and $\text{TMT}(Z)$ from such minimum spanning trees.
3. Compute F using $\text{TMT}(X)$ and $\text{TMT}(Z)$.
4. Perform a Gaussian-column reduction of F .

Notice that Steps 1 and 4 can be performed by standard methods that are widely well-known, so we do not discuss them. Thus, we differ a detailed explanation of Steps 2 and 3 to the following subsection. Now, we consider an example.

Example 3.1. *In this example, we check that the matching from Example 2.12 for the pair $X \subseteq Z$ coincides with the one obtained by the above-mentioned matrix procedure.*

First, suppose we have computed F the associated matrix to $f : \text{PH}(X) \rightarrow \text{PH}(Z)$ where the entries are sorted from lower to higher endpoint, that is,

the rows correspond to the endpoints 0.05, 0.05, 1, 03, 1.11 and 1.19 of the intervals of $B(U)$ and the columns correspond to the endpoints 1.19 and 2.24 of the intervals of $B(V)$. Then, we compute the reduced matrix R obtained using left-to-right column additions:

$$F = \begin{bmatrix} 0 & 0 \\ 0 & 0 \\ 0 & 0 \\ 1 & 0 \\ 1 & 1 \end{bmatrix} \longrightarrow R = \begin{bmatrix} 0 & 0 \\ 0 & 0 \\ 0 & 0 \\ 1 & 1 \\ 1 & 0 \end{bmatrix}$$

In particular, notice that the reduced matrix R has pivots in the last two rows that correspond to pairing the two intervals of S^V with the two longest intervals of S^U , obtaining $\mathcal{M}_f^0(1.19, 1.19) = 1$ and $\mathcal{M}_f^0(2.24, 1.11) = 1$.

3.2. Associated matrix F computation

Here, we introduce a procedure to obtain the matrix F associated to $(\beta^{-1}f\alpha)_0$, ignoring the term $(\kappa_\infty)_0 \rightarrow (\kappa_\infty)_0$. As outlined in Subsection 3.1, to compute F , first we need to execute Step 1 and compute the minimum spanning trees $\text{MST}(X)$ and $\text{MST}(Z)$ of $\text{VR}(X)$ and $\text{VR}(Z)$, which we assume is already done.

Let us now focus on Step 2 that computes the triplet merge trees $\text{TMT}(X)$ and $\text{TMT}(Z)$.

First of all, notice that, if Step 1 is performed using Kruskal's method, one could inspect the union-find data structures to directly produce $\text{TMT}(X)$ and $\text{TMT}(Z)$. Unfortunately, usual implementations of minimum spanning trees do not provide access to such union-find data structures. It is worth pointing out that Steps 1 and 2 could also be directly obtained from using the very efficient implementation from [12]. However, for the sake of flexibility, we believe it is beneficial to compute the triplet merge trees from any previous computation of minimum spanning trees independently of the method used.

Next, we describe how to execute Step 2 in a lightweight and efficient manner, which is (yet) another adaptation of Kruskal's algorithm that allows us to implement computations of triplet merge trees in a short Python script with few requirements.

We start by considering $\text{TMT}(Z)$ to be an empty set. Also, we consider a vector C of length n . The i -coordinate of C will be denoted as $C[i]$. Initially, $C = (0, 1, \dots, n - 1)$.

Next, we iterate over increasing values $b > 0$. For each b , we set E_b as the set of edges from $\text{MST}(Z)$ of length b . Then, while $E_b \neq \emptyset$, we do the following operations:

- (i) Take an edge $[z_i, z_j] \in E_b$ such that $\min\{C[i], C[j]\}$ is as small as possible; if there is more than one such edge, pick any;
- (ii) set $m \leftarrow \min\{C[i], C[j]\}$ and $M \leftarrow \max\{C[i], C[j]\}$;
- (iii) add the triplet (z_M, b, z_m) to $\text{TMT}(Z)$, (here notice that $m < M$ since otherwise $\text{MST}(Z)$ would not be a tree);
- (iv) range over $k \in \llbracket n \rrbracket$ and if $C[k] = M$ then set $C[k] \leftarrow m$.
- (v) remove (z_i, z_j) from E_b .

Then, we continue iterating over increasing values $b > 0$. Notice that, at the end of the iteration over a fixed $b > 0$, for each point, $z_i \in Z$, the entry $C[i]$ is equal to the minimum index in $A_b(z_i)$; were $A_b(z_i)$ is the connected component in $\text{VR}_r(Z)$ that contains z_i . We obtain $\text{TMT}(X)$ by performing the same procedure on $\text{MST}(X)$. The complexity of this step is $\mathcal{O}(n \log n)$ since it is an adaptation of Kruskal's algorithm and $\text{MST}(Z)$ has $n - 1$ edges being $n = \#Z$.

Here, we obtain a result that justifies that our procedure leads to $\text{TMT}(Z)$. In addition, we need this result for Proposition 5.5.

Proposition 3.2. *Denote by $\text{MST}_b(Z)$ the subtree of $\text{TMT}(Z)$ containing the edges of length $\leq b$ and denote by $E(\text{MST}(Z))$ the set of edges of $\text{MST}(Z)$. Given $(z_j, b, z_i) \in \text{TMT}(Z)$, we have that z_i and z_j lie in the same component in $\text{MST}_b(Z)$, which is represented by z_j . Furthermore, there exists a bijection $\alpha : \text{TMT}(Z) \rightarrow E(\text{MST}(Z))$ such that, given $(z_j, b, z_i) \in \text{TMT}(Z)$,*

1. *the edge $\alpha((z_j, b, z_i))$ has length b and*
2. *z_i and z_j are not path connected in $\text{MST}(Z) \setminus \{\alpha((z_j, b, z_i))\}$.*

PROOF. We consider the algorithm for computing $\text{TMT}(Z)$ from $\text{MST}(Z)$ outlined above and consider the iteration step at value $b > 0$. Recall that we iterate over edges (z_i, z_j) in E_b adding triplets (z_M, b, z_m) to $\text{TMT}(Z)$. Now, by Steps (i) and (iv), the value m can only increase as we iterate over

E_b . This implies that z_M and z_m lie in the same connected component in $\text{MST}_b(Z)$ represented by z_m .

Next, we show the second claim. Consider again the iteration step at value b , where we range over edges (z_i, z_j) in E_b adding triplets (z_M, b, z_m) to $\text{TMT}(Z)$. This implies that there exists a path γ in $\text{MST}_b(Z)$ joining z_M and z_m and having (z_i, z_j) as an edge. We set $\alpha((z_M, b, z_m)) = (z_i, z_j)$. Now, z_i and z_j are not path connected in $\text{MST}(Z) \setminus \{\alpha((z_M, b, z_m))\}$ since otherwise $\text{MST}(Z)$ could not be a tree. \square

Now we focus on Step 3 that computes the matrix F associated to $(\beta^{-1}f\alpha)_0$.

Notice that one could compute F from Step 1 by using the first differential matrices from $\text{MST}(X)$ and $\text{MST}(Z)$. However, the advantage of using triplet merge trees is that it leads to a faster Gaussian reduction because the matrices involved have fewer rows.

We first consider the canonical basis for $V_0 = H_0(\text{VR}_0(X))$ where generators correspond to points from X . On the other hand, we denote by A_0 the matrix associated with α_0 ignoring the summand $(\kappa_\infty)_0$. That is, A_0 has rows indexed by X and columns indexed by $\text{TMT}(X)$, where the (z_j, b, z_i) -column has non-trivial entries in the positions i and j .

Next, we consider the canonical basis for $U_0 = H_0(\text{VR}_0(Z))$ given by points from Z . Further, U_0 can be decomposed into a direct sum $U_0 = U_0^X \oplus U_0^{Z \setminus X}$ where U_0^X is generated by the points from X and $U_0^{Z \setminus X}$ is generated by the points from $Z \setminus X$. We define $\text{TMT}(X, Z)$ to be the subset of $\text{TMT}(Z)$ given by triplets (z_j, b, z_i) such that $i < j < \ell$; so that $z_i, z_j \in X$ by hypotheses. Now, consider the following linear map,

$$\beta_0^X : \left(\bigoplus_{(z_j, b, z_i) \in \text{TMT}(X, Z)} (\kappa_b)_0 \right) \oplus (\kappa_\infty)_0 \rightarrow U_0^X.$$

which is a restriction of β_0 , and so it is injective. Further, β_0^X is a bijection since $\#\text{TMT}(X, Z) = \#X - 1$. Now, we denote by B_0 the associated matrix to β_0^X ignoring the $(\kappa_\infty)_0$ component. That is, B_0 has rows indexed by X and columns indexed by $\text{TMT}(X, Z)$, where the (z_j, b, z_i) -column has non-trivial entries in the positions i and j .

Next, as f_0 is induced by the inclusion $X \subseteq Z$, we have that f_0 is equal to $f_0^X : V_0 \rightarrow U_0^X$ composed with the inclusion $\iota_U^X : U_0^X \hookrightarrow U_0$. We denote by F^X the matrix associated to $(\beta_0^X)^{-1} \circ f_0^X \circ \alpha_0$, ignoring the terms $(\kappa_\infty)_0$. By our definitions, it follows that $F^X = (B_0)^{-1}A_0$. Adding zero rows corresponding

to triples in $\text{TMT}(Z) \setminus \text{TMT}(X, Z)$ to F^X , we obtain F . To see why, notice that there is a commutative diagram

$$\begin{array}{ccccc}
& & \left(\bigoplus_{(z_j, b, z_i) \in \text{TMT}(X)} (\kappa_b)_0 \right) \oplus (\kappa_\infty)_0 & & \\
& \swarrow \alpha_0 & & & \\
V_0 & \xrightarrow{f_0} & U_0 & \xrightarrow{(\beta_0)^{-1}} & \left(\bigoplus_{(z_j, b, z_i) \in \text{TMT}(Z)} (\kappa_b)_0 \right) \oplus (\kappa_\infty)_0 \\
& \searrow f_0^X & \uparrow \iota_U^X & & \uparrow \iota_{\text{TMT}}^X \\
& & U_0^X & \xrightarrow{(\beta_0^X)^{-1}} & \left(\bigoplus_{(z_j, b, z_i) \in \text{TMT}(X, Z)} (\kappa_b)_0 \right) \oplus (\kappa_\infty)_0
\end{array}$$

where ι_{TMT}^X is induced by the inclusion $\text{TMT}(X, Z) \subseteq \text{TMT}(Z)$.

Now, we explain how to compute $F^X = (B_0)^{-1}A_0$. We consider the block matrix below, which we reduce via left-to-right column additions:

$$\begin{pmatrix} \text{id} & \mathbf{0} \\ \mathbf{0} & \text{id} \\ B_0 & A_0 \end{pmatrix} \mapsto \begin{pmatrix} \text{id} & F^X \\ \mathbf{0} & \text{id} \\ B_0 & \mathbf{0} \end{pmatrix}$$

where id is the identity matrix and $\mathbf{0}$ is the zero matrix. Notice that the pivots from B_0 are all unique, which allows a quick search for columns corresponding to pivots. The result obtained from the upper right corner of the reduced block matrix corresponds to the first ℓ rows, and the last ℓ columns equals F^X . The worst-case complexity of this reduction is about $\mathcal{O}(\ell^3)$, where $\ell = \#X$, since we have to reduce the matrix A_0 which is a $(\ell \times \ell)$ -matrix, by adding the columns from B_0 , which has already been reduced. In practice, the computation time is reduced since the matrices we deal with are sparse.

Example 3.3. *In this example, we explain how to compute the matrix F that we used in Example 3.1. Recall the descriptions of $\text{TMT}(X)$ and $\text{TMT}(Z)$ from Examples 2.4 and 2.7. Then, we might write B_0 , A_0 , and F^X as follows*

$$B_0 = \begin{bmatrix} 0 & 1 \\ 1 & 1 \\ 1 & 0 \end{bmatrix}, \quad A_0 = \begin{bmatrix} 1 & 1 \\ 0 & 1 \\ 1 & 0 \end{bmatrix} \quad \text{and} \quad F^X = \begin{bmatrix} 1 & 0 \\ 1 & 1 \end{bmatrix}$$

where, B_0 has rows indexes by $X = \{z_0, z_1, z_2\}$ and columns indexed by $\text{TMT}(X, Z) = \{(z_2, 1.11, z_1), (z_1, 1.19, z_0)\}$, which correspond to the last two

triplets from $\text{TMT}(Z)$, and A_0 has rows indexes by X and columns indexes by $\text{TMT}(X) = \{(z_2, 1.19, z_0), (z_1, 2.24, z_0)\}$. Then, F is obtained by adding $3 = (\#Z) - (\#X)$ trivial rows on top of F^X , as can be checked in Example 3.1.

Now, we give an estimate of the complexity of our procedure. We already have discussed the complexity of Steps 2 and 3, so we first discuss the complexity of the remaining steps. For Step 1, since the number of edges in $\text{VR}(Z)$ is about n^2 , where $n = \#Z$, we can use the standard complexity of computing minimum spanning trees to obtain a complexity of $\mathcal{O}(n^2 \log n^2)$. Now, for Step 4, the worst case complexity for the Gaussian elimination of F is $\mathcal{O}(\ell^3)$, where $\ell = \#X$, since F is a $(n \times \ell)$ -matrix with $n - \ell$ trivial rows. Overall, the worst-time complexity of the four terms in the procedure is $\mathcal{O}(n^2 \log n^2 + n \log n + \ell^3 + \ell^3)$ which simplifies to $\mathcal{O}(n^2 \log n + \ell^3)$. In our experiments, the computation of Step 1 takes the most time since usually, $\#Z$ is much larger than $\#X$. For example, in Table 1, random sets of different sizes and dimensions were generated, and the time of execution of the proposed algorithm was given. We can see that the time performance mainly depends on the size of the dataset considered and the size of the subset. Furthermore, those times could be optimized in the future, considering the particular structures of the matrices we deal with.

4. Properties and stability of the induced block function \mathcal{M}_f^0

In this section, we investigate the distinctive properties of \mathcal{M}_f^0 , which arise from the fact that we work with finite metric spaces $X \subseteq Z$ and that all the intervals of the barcodes we consider start at zero. Later, we introduce a diagram representation for \mathcal{M}_f^0 analogous to persistence diagrams and study its most significant differences. Finally, we study the stability of the block function \mathcal{M}_f^0 that will provide robustness to the concept of topological data quality via matchings proposed in Section 5.

4.1. Ladder module decompositions and \mathcal{M}_f^0

In this subsection, we inspect the particular properties of \mathcal{M}_f^0 that come from the fact that f is a morphism between persistence modules whose barcodes are composed of intervals that start at zero. This implies that \mathcal{M}_f^0 has very close relations to the image, kernel and cokernel of f .

Size	Prop	Time (s) Dim 100	Time (s) Dim 200	Time (s) Dim 500	Time (s) Dim 1000
1000	0.1	0.2137	0.2251	0.2906	0.4167
	0.2	0.2205	0.2337	0.3025	0.4266
	0.5	0.2614	0.2770	0.3672	0.5181
	0.8	0.3420	0.3647	0.4785	0.6791
5000	0.1	6.8683	7.4391	9.3776	13.2139
	0.2	7.1100	7.6029	9.6264	13.5654
	0.5	8.3384	9.0599	11.3875	15.9382
	0.8	11.0920	11.9642	15.1606	21.0903
10000	0.1	30.9312	33.8928	43.3496	59.5236
	0.2	31.7921	34.5644	44.4252	61.1580
	0.5	37.6867	41.3084	52.5283	72.4249
	0.8	50.1831	54.3484	69.9975	96.1254

Table 1: Random sets were generated for different dimensions and sizes. Then, random subsets taking different proportions of the datasets were chosen, and the matching was computed. The values given are the execution time in seconds for the computation of F .

Proposition 4.1. *Given a finite metric space Z and $X \subseteq Z$, consider the induced morphism $f : V \rightarrow U$, where $V = \text{PH}_0(X)$ and $U = \text{PH}_0(Z)$. Then,*

$$f \simeq \left(\bigoplus_{b>0} \bigoplus_{a \geq b} \bigoplus_{s \in \llbracket \mathcal{M}_f^0(a,b) \rrbracket} (\kappa_a \rightarrow \kappa_b) \right) \oplus \left(\bigoplus_{b>0} \bigoplus_{s \in \llbracket N_f(b) \rrbracket} (0 \rightarrow \kappa_b) \right) \oplus (\kappa_\infty \rightarrow \kappa_\infty) \quad (3)$$

where $N_f(b) = m^U(b) - \sum_{a>0} \mathcal{M}_f^0(a,b)$, and $m^U(b)$ denotes the multiplicity of $[0, b]$ in $B(U)$.

PROOF. By Lemma 2.9, there are integers $r_a^b \geq 0$ and $d_a^+, d_b^- \geq 0$ such that

$$f \simeq \left(\bigoplus_{b>0} \bigoplus_{a \geq b} \bigoplus_{s \in \llbracket r_a^b \rrbracket} (\kappa_a \rightarrow \kappa_b) \right) \oplus \left(\bigoplus_{b>0} \bigoplus_{s \in \llbracket d_b^- \rrbracket} (0 \rightarrow \kappa_b) \right) \oplus \left(\bigoplus_{a>0} \bigoplus_{s \in \llbracket d_b^+ \rrbracket} (\kappa_a \rightarrow 0) \right) \oplus (\kappa_\infty \rightarrow \kappa_\infty).$$

Now, by Lemma 2.11, the block function \mathcal{M}_f^0 induces a partial matching. Since \mathcal{M}_f^0 is linear with respect to direct sums and, by Proposition 2.13,

$\mathcal{M}_{\kappa_a \rightarrow \kappa_b}^0(a, b) = 1$, it follows that $\mathcal{M}_f^0(a, b) = r_a^b$ for all $a \geq b > 0$. On the other hand, it also follows that $d_b^- = N_f(b)$ since there must be as many copies as $m^U(b)$ in the codomain of f . Finally, since there is an inclusion $X \subseteq Z$, the induced map $f_0 : H_0(\text{VR}_0(X)) \rightarrow H_0(\text{VR}_0(Z))$ is an injection. This implies that $d_a^+ = 0$ for all $a > 0$, since otherwise f_0 would not be injective. Altogether we obtain (3). \square

Example 4.2. Consider again Example 3.1. By the computed induced block function \mathcal{M}_f^0 and by Proposition 4.1 we obtain the following isomorphism

$$f \simeq (\kappa_{1.19} \rightarrow \kappa_{1.19}) \oplus (\kappa_{2.24} \rightarrow \kappa_{1.11}) \oplus (0 \rightarrow \kappa_{1.03}) \\ \oplus (0 \rightarrow \kappa_{0.50}) \oplus (0 \rightarrow \kappa_{0.50}) \oplus (\kappa_\infty \rightarrow \kappa_\infty)$$

since $\mathcal{M}_f^0(1.19, 1.19) = \mathcal{M}_f^0(2.24, 1.11) = 1$, $N_f(1.03) = 1$ and $N_f(0.50) = 2$.

An immediate consequence of Proposition 4.1 is that (1) is an equality since there are no unmatched intervals by \mathcal{M}_f^0 . Furthermore, Proposition 4.1 also implies that \mathcal{M}_f^0 always induces an injective assignment $\sigma^f : \text{Rep B}(V) \hookrightarrow \text{Rep B}(U)$. Also, notice that Proposition 4.1 gives an alternative definition for \mathcal{M}_f^0 :

$$\mathcal{M}_f^0(a, b) = \# \left\{ \text{summands } \kappa_a \rightarrow \kappa_b \text{ in the decomposition of } f \right\}.$$

Besides, \mathcal{M}_f^0 has a direct relation with the persistence modules $\ker(f)$, $\text{coker}(f)$ and $\text{im}(f)$.

Proposition 4.3. There are the following isomorphisms:

$$\text{im}(f) \simeq \left(\bigoplus_{b>0} \bigoplus_{a \geq b} \bigoplus_{s \in \llbracket \mathcal{M}_f^0(a, b) \rrbracket} \kappa_b \right) \oplus \kappa_\infty,$$

$$\ker(f) \simeq \bigoplus_{b>0} \bigoplus_{a>b} \bigoplus_{s \in \llbracket \mathcal{M}_f^0(a, b) \rrbracket} \kappa_{[b, a]},$$

and also $\text{coker}(f) \simeq \bigoplus_{b>0} \bigoplus_{s \in \llbracket N_f(b) \rrbracket} \kappa_b$.

PROOF. We prove the isomorphism for $\ker(f)$ as the other two are analogous. First, notice that since $a \geq b$ then $\ker(\kappa_a \rightarrow \kappa_b) = \kappa_{[a, b]}$ while $\ker(0 \rightarrow \kappa_b) =$

0 for all $b > 0$. Now, by Proposition 4.1 as well as commutativity of \ker with direct sums, we have the following isomorphisms and equalities

$$\begin{aligned}
\ker(f) &\simeq \left(\bigoplus_{>0} \bigoplus_{a \geq b} \bigoplus_{s \in \llbracket \mathcal{M}_f^0(a,b) \rrbracket} \ker(\kappa_a \rightarrow \kappa_b) \right) \\
&\quad \oplus \left(\bigoplus_{b > 0} \bigoplus_{s \in N_f(b)} \ker(0 \rightarrow \kappa_b) \right) \\
&= \bigoplus_{b > 0} \bigoplus_{a \geq b} \bigoplus_{s \in \llbracket \mathcal{M}_f^0(a,b) \rrbracket} \kappa_{[b,a]} \\
&= \bigoplus_{b > 0} \bigoplus_{a > b} \bigoplus_{s \in \llbracket \mathcal{M}_f^0(a,b) \rrbracket} \kappa_{[b,a]}. \quad \square
\end{aligned}$$

In particular, notice that \mathcal{M}_f^0 is determined by the barcodes $B(\ker(f))$ and $B(V)$. This can be done using the equality $\mathcal{M}_f^0(a, b) = m^{\ker(f)}([b, a])$ for all $a > b$ and also $\mathcal{M}_f^0(a, a) = m^V(a) - \sum_{b < a} \mathcal{M}_f^0(a, b)$ for all $a > 0$.

4.2. 0-persistence matching diagrams

In this subsection, we briefly introduce a diagram representation for \mathcal{M}_f , which is analogous to persistence diagrams but with some fundamental differences.

Now, we define the *0-persistence matching diagram* (also called *matching diagram*, for short) $D(f)$ to be the multiset $(S^{D(f)}, m^{D(f)})$ given by a set $S^{D(f)} \subset \overline{\mathbb{R}} \times \mathbb{R}$, where $\overline{\mathbb{R}} = \mathbb{R} \cup \{\infty\}$, together with the multiplicity function $m^{D(f)}$ given by $m^{D(f)}((a, b)) = \mathcal{M}_f^0(a, b)$ for all pairs $(a, b) \in \mathbb{R} \times \mathbb{R}$ and $m^{D(f)}((\infty, b)) = N_f(b)$ for all $b > 0$. Notice that if $(a, b) \in S^{D(f)}$ then $b \leq a$.

Example 4.4. We consider \mathcal{M}_f^0 from Example 2.12. In this case, one can compute the matching diagram $D(f) = (S^{D(f)}, m^{D(f)})$ and plot the points from $S^{D(f)}$ as done in Figure 5. Notice that the pairs $(\infty, b) \in S^{D(f)}$ have been plotted over a vertical blue line with the sign ∞ next to it. Also, since $N_f(0.50) = 2$ then $(\infty, 0.50) \in S^{D(f)}$ has multiplicity 2, that is, $m^{D(f)}((\infty, 0.50)) = 2$; all other points have multiplicity 1.

An advantage of using the multiset $D(f)$ is that it contains all information from the five multisets $B(V)$, $B(U)$, $B(\ker(f))$, $B(\text{im}(f))$ and $B(\text{coker}(f))$. Using Propositions 4.1 and 4.3 together with the definition of $D(f)$ we show the claim for each case:

Remark 4.5. Let $D(f) = (S^{D(f)}, m^{D(f)})$. Then,

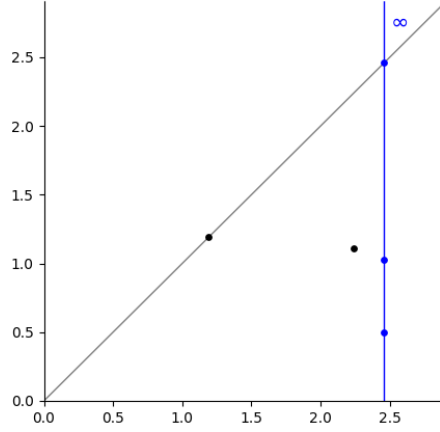


Figure 5: Depiction of the set $S^{D(f)}$ associated to the matching diagram $D(f)$.

(1) setting $B(V) = (S^V, m^V)$, we have

$$S^V = \{[0, a) \text{ such that } \exists(a, b) \in S^{D(f)} \text{ with } 0 < a < \infty\}$$

and, given $0 < a < \infty$, $m^V(a) = \sum_{b \leq a} m^{D(f)}((a, b))$;

(2) similarly, given $B(U) = (S^U, m^U)$ we have

$$S^U = \{[0, b) \text{ such that } \exists(a, b) \in S^{D(f)} \text{ with } b < \infty \text{ and } b \leq a \leq \infty\}$$

and also $m^U(b) = \sum_{b \leq a \leq \infty} m^{D(f)}((a, b))$.

(3) Given $B(\ker(f)) = (S^{\ker(f)}, m^{\ker(f)})$ we have

$$S^{\ker(f)} = \{[b, a) \text{ such that } \exists(a, b) \in S^{D(f)} \text{ with } b < a < \infty\}$$

and also $m^{\ker(f)}([b, a)) = m^{D(f)}((a, b))$.

(4) given $B(\text{im}(f)) = (S^{\text{im}(f)}, m^{\text{im}(f)})$ we have

$$S^{\text{im}(f)} = \{[0, b) \text{ such that } \exists(a, b) \in S^{D(f)} \text{ with } b \leq a < \infty\}$$

and also $m^{\text{im}(f)}(b) = \sum_{b \leq a < \infty} m^{D(f)}((a, b))$ for $b < \infty$.

(5) given $B(\text{coker}(f)) = (S^{\text{coker}(f)}, m^{\text{coker}(f)})$ we have

$$S^{\text{coker}(f)} = \{[0, b) \text{ such that } \exists(\infty, b) \in S^{D(f)}\}$$

$$\text{and also } m^{\text{coker}(f)}([0, b) = m^{D(f)}((\infty, b)).$$

Conversely, we might write $D(f)$ in terms of $B(\ker(f))$, $B(V)$ and $B(\text{coker}(f))$. This is followed by setting

$$\begin{aligned} S^{D(f)} = & \{(a, b) \text{ such that } [b, a) \in S^{\ker(f)}\} \\ & \cup \{(a, a) \text{ such that } a < \infty \text{ and } m^V(a) > \sum_{b < a} m^{\ker(f)}([b, a))\} \\ & \cup \{(\infty, b) \text{ such that } [0, b) \in S^{\text{coker}(f)}\} \end{aligned}$$

and also

$$m^{D(f)}((a, b)) = \begin{cases} m^{\ker(f)}([b, a)) & \text{if } b < a < \infty, \\ m^V(a) - \sum_{r < a} m^{\ker(f)}([r, a)) & \text{if } b = a < \infty, \\ m^{\text{coker}(f)}(b) & \text{if } b < a = \infty. \end{cases}$$

4.3. Stability of \mathcal{M}_f^0

In this subsection, we find an upper bound for the stability of \mathcal{M}_f^0 . Intuitively, by the stability of \mathcal{M}_f^0 we mean that considering the pair of samples $X \subseteq Z$ and moving their positions slightly, so that we obtain a new pair $X' \subseteq Z'$, then the induced matchings \mathcal{M}_f^0 and $\mathcal{M}_{f'}^0$ are approximately “the same”, where $f' : \text{PH}_0(X') \rightarrow \text{PH}_0(Z')$. In particular, we show the stability of $D(f)$, which, by its definition, is equivalent to showing the stability of \mathcal{M}_f^0 , but it is easier to formulate.

Theorem 4.6. *Consider finite metric spaces $X \subseteq Z$ and $X' \subseteq Z'$ such that $d_{GH}((X, Z), (X', Z')) < \varepsilon$. Then there exists a partial matching $\sigma^{D(f)} : \text{Rep } D(f) \rightarrow \text{Rep } D(f')$ such that*

- for $((a, b), i) \in \text{coim}(\sigma^{D(f)})$, writing $\sigma^{D(f)}((a, b), i) = ((a', b'), j)$, we have that (either $a = a' = \infty$ or $|a - a'| < 2\varepsilon$) and $|b - b'| < 2\varepsilon$.
- for $((a, b), i) \in \text{Rep } D(f) \setminus \text{coim}(\sigma^{D(f)})$ then (either $a = \infty$ or $a < 2\varepsilon$) and $b < 2\varepsilon$.

- for $((a', b'), j) \in \text{Rep } D(f') \setminus \text{im}(\sigma^{D(f)})$ then (either $a' = \infty$ or $a' < 2\varepsilon$) and $b' < 2\varepsilon$.

The proof of this theorem, which is quite technical, is elaborated in detail in Appendix Appendix B.

Example 4.7. Consider the pair $X \subset Z$ from Example 2.3 together with the matching diagram $D(f)$ from Example 4.4. Also, consider $X' \subseteq Z'$ such that $d_H(Z, Z') < \varepsilon$ and $d_H(X, X') < \varepsilon$ for $\varepsilon \sim 0.27$. In Subfigure (6a), we plot Z in blue and Z' in red, and we plot the points of X and X' using circles while the remaining points are marked with \times signs. In the same subfigure, we pair the points from Z with the closest ones from Z' by connecting them with lines; this matches points from X with points from X' . Now, in Subfigure (6b), we plot, in a superposed manner, the matching diagrams $D(f)$ and $D(f')$, respectively. We can observe that there is a partial matching $\sigma^{D(f)}: D(f) \dashrightarrow D(f')$ that is bounded by ε . More concretely, we have $D(f) = \{S^{D(f)}, m^{D(f)}\}$ and $D(f') = \{S^{D(f')}, m^{D(f')}\}$ where the pairs $(a, b) \in S^{D(f)}$ and $(a', b') \in S^{D(f')}$ range over the values in the table below (where values are rounded to two decimals):

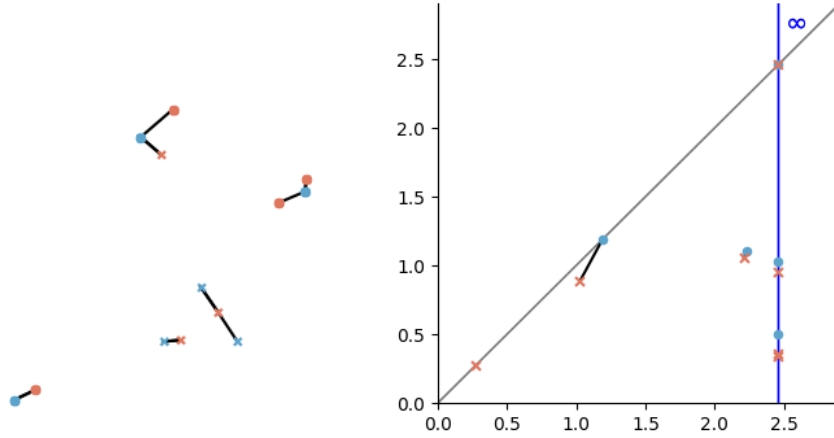
a	b	a'	b'	$ a - a' $	$ b - b' $
1.19	1.19	1.03	0.89	0.16	0.30
2.24	1.11	2.21	1.06	0.02	0.05
—	—	0.27	0.27	—	—
<i>inf</i>	1.03	<i>inf</i>	0.95	<i>nan</i>	0.07
<i>inf</i>	0.50	<i>inf</i>	0.36	<i>nan</i>	0.14
<i>inf</i>	0.50	<i>inf</i>	0.34	<i>nan</i>	0.16

Further, in this table, in each row, a couple of pairs of values (a, b) and (a', b') are matched, and the differences between their endpoints are shown on the right hand of the table. Notice that the maximum value is 0.3, so the stability bound is satisfied since $0.30 < 0.54$. In Subfigure (6b), we depict such matching by connecting segments.

Finally, notice that our stability result implies that the “noise” on $D(f)$ lies around the points $(0, 0)$ and $(\infty, 0)$.

5. Topological Data Quality via Matchings

In this section, we interpret the matching \mathcal{M}_f^0 , giving an intuition of the relation between X and Z . In particular, we study the interpretation of \mathcal{M}_f^0



(a) $X \subset Z$ (in red) and $X' \subset Z'$ (in blue). (b) $D(f)$ (in red) and $D(f')$ (in blue).

Figure 6: Illustration of the stability of matching diagrams. On the left, we show two pairs (X, Z) and (X', Z') and the matching that provides the value of $d_{GH}((X, Z), (X', Z'))$. The matching diagrams $D(f)$ and $D(f')$ associated to $X \subset Z$ and $X' \subset Z'$, respectively, are depicted on the right with the partial matching $\sigma^{D(f)}$.

to know whether X “represents well” the clusters from $\text{VR}_r(Z)$ for $r \geq 0$. Additionally, we provide bounds to the Hausdorff distance between X and Z from \mathcal{M}_f^0 .

5.1. Topological Data Quality

Here, using \mathcal{M}_f^0 , we want to answer the following three questions, given a fixed r :

- Q1. How many $\text{VR}_r(Z)$ components have at least a sample from X ?
- Q2. How many components from $\text{VR}_r(X)$ are not components in $\text{VR}_r(Z)$?
- Q3. How many components from $\text{VR}_r(Z)$ have no samples from X ?

To start, notice that these questions have a direct interpretation in terms of the image, kernel and cokernel from $f : V \rightarrow U$, for $V = \text{PH}_0(X)$ and $U = \text{PH}_0(Z)$. In particular, we have the following result.

Proposition 5.1. *Consider the linear map $f_r : V_r \rightarrow U_r$, where $V_r = \text{H}_0(\text{VR}_r(X))$ and $U_r = \text{H}_0(\text{VR}_r(Z))$, for $X \subseteq Z$ and for a given value $r \geq 0$. The following holds:*

- A1. $\dim(\text{im}(f_r))$ is the number of components from $\text{VR}_r(Z)$ that have at least a sample from X .
- A2. $\dim(\text{ker}(f_r))$ is the number of components from $\text{VR}_r(X)$ that are not components in $\text{VR}_r(Z)$.
- A3. $\dim(\text{coker}(f_r))$ is the number of components from $\text{VR}_r(Z)$ that have no samples from X .

PROOF. For ease, we assume that $X = \{z_0, \dots, z_{\ell-1}\}$ and also $Z \setminus X = \{z_\ell, \dots, z_{n-1}\}$. Next, recall the set $\pi_0(\text{VR}_r(Z))$ of connected components from $\text{VR}_r(Z)$ labelled by the vertices with smaller indexes. With these conventions, the $\pi_0(\text{VR}_r(Z))$ labels provide valuable information. Namely, given $\alpha_r \in \pi_0(\text{VR}_r(Z))$ associated to a connected component A_r in $\text{VR}(Z)$ represented by the vertex $z_j \in A_r$ with the lowest label, there are two options:

- If $j \leq \ell$ then A_r contains at least one point from X .
- If $\ell < j$ then A_r does not contain points from X .

In addition, given two elements $[z_k], [z_i] \in \pi_0(\text{VR}_r(X))$ for some $i < k$ and such that $f_r([z_k]) = f_r([z_i])$, then the two different connected components labelled by z_k and z_i from $\text{VR}_r(X)$ embed into the same connected component in $\text{VR}_r(Z)$. \square

Next, we relate the image, kernel and cokernel dimensions of f with the matching \mathcal{M}_f^0 .

Proposition 5.2. *Given $X \subseteq Z$, consider the persistence morphism $f : V \rightarrow U$ for $V = \text{PH}_0(X)$ and $U = \text{PH}_0(Z)$. The following equalities hold:*

- $\#X = \sum_{b>0} \sum_{a \geq b} \mathcal{M}_f(a, b)$
- $\#Z - \#X = \sum_{b>0} N_f(b)$
- $\dim(\text{im}(f_r)) = \#X - \sum_{b \leq r} \sum_{a \geq b} \mathcal{M}_f(a, b)$
- $\dim(\text{ker}(f_r)) = \sum_{b \leq r} \sum_{a > r} \mathcal{M}_f(a, b)$
- $\dim(\text{coker}(f_r)) = \#Z - \#X - \sum_{b \leq r} N_f(b)$

PROOF. This follows from Remark 4.5. \square

Now we consider the following quantity

$$\eta_f = \max_{b \geq 0} \{ b \mid N_f(b) > 0 \text{ or } b = 0 \}.$$

which is the endpoint of the largest interval $[0, b)$ of S^U such that there exist j with $([0, b), j) \in \text{Rep B}(U)$ not matched by σ^f ; if there exist no such intervals, we set $\eta_f = 0$. The following result guarantees that all $\text{VR}_r(Z)$ components are represented by X .

Proposition 5.3. *All components from $\text{VR}_r(Z)$ contain points from X for all $r \geq \eta_f$. In particular, if $\eta_f = 0$, then $X = Z$.*

PROOF. By hypothesis and Proposition 5.2, it follows that

$$\#Z - \#X = \sum_{b > 0} N_f(b) = \sum_{b < \eta_f} N_f(b)$$

and so $\dim(\text{coker}(f_r)) = 0$ for all $r \geq \eta_f$. Hence, the first claim follows by applying Proposition 5.1.

In particular, if $\eta_f = 0$ then $\dim(\text{coker}(f_0)) = 0$, which implies that all components from $\text{VR}_0(Z) = Z$ have samples from X . Thus, since Z is a metric space, it follows that $X = Z$. \square

5.2. Hausdorff distance bounds from matchings

In this subsection, we obtain a couple of bounds to the Hausdorff distance $d_H^Z(X, Z)$ between a subset X and the metric space Z . The first, which is the weaker, is solely based on \mathcal{M}_f^0 . The second also uses the computed information from $\text{TMT}(Z)$ to deduce a sharper bound obtained with the computation of \mathcal{M}_f^0 described in this work. The first bound relates the points from the infinity line of $D(f)$ with the Hausdorff distance.

Proposition 5.4. $\eta_f \leq d_H^Z(X, Z) \leq \sum_{b > 0} N_f(b)b$.

PROOF. Here, we prove the lower bound, leaving the upper bound as a consequence of Proposition 5.5. Now, for all $r < \eta_f$, by Proposition 5.1 and Proposition 5.2 there exists at least one component from $\text{VR}_r(Z)$ with no samples from X . In particular, there exists at least one point $z \in Z \setminus X$ such that $d^Z(z, X) > r$. Hence $\eta_f \leq d^Z(z, X)$ and the lower bound follows, since $d^Z(z, X) \leq d_H^Z(X, Z)$. \square

Next, we define a quantity that can be obtained using $\text{TMT}(Z)$: Let c_f denote the maximum number of points from $Z \setminus X$ contained in a single connected component from $\text{VR}_{\eta_f}(Z)$. In addition, assuming $\eta_f \neq 0$, we denote

$$b_f = \max\{b > 0 \text{ such that } \sum_{r \geq b} N_f(r) \geq c_f\}$$

and also $r_f = \sum_{b > b_f} N_f(b) - c_f$, noticing that $b_f > 0$ and $0 \leq r_f < N_f(b_f)$. Then, we obtain the following bound.

Proposition 5.5. $d_H^Z(X, Z) \leq \left(\sum_{b > b_f} N_f(b)b \right) - r_f b_f \leq \sum_{b > 0} N_f(b)b$.

PROOF. We focus on the first inequality since the second is direct. Suppose that we have computed $\text{MST}(Z)$ and $\text{TMT}(Z)$ as directed in Subsection 3.1. In particular, we consider the bijection α sending triplets from $\text{TMT}(Z)$ to edges in $\text{MST}(Z)$ from Proposition 3.2. Now, consider a point $z_i \in Z \setminus X$. By definition, there exists a path (with no cycles) γ in $\text{MST}(Z)$ connecting z_i with a point in X and such that all edges have length $\leq \eta_f$. Now, if it exists, we take any edge e from γ such that $e = \alpha((z_j, b, z_k))$ for $(z_j, b, z_k) \in \text{TMT}(X, Z)$. If such e does not exist, then fix γ . Otherwise, we modify γ as follows. By Proposition 3.2, there exists a path τ in $\text{MST}(Z)$ such that its edges have length $b \leq \eta_f$, it starts at z_j and ends at z_k , and it goes along the edge e . We combine γ with τ to obtain a new path γ' which joins z_i with either z_j or z_k in such a way that e is not in γ' . Now, we look again for any edge (if it exists) e' in $\text{MST}(Z)$ such that $e' = \alpha((z_n, b, z_m))$ for $(z_n, b, z_m) \in \text{TMT}(X, Z)$ and modify again γ' if necessary. Now, as we iterate, we cannot consider the same edge from $\alpha(\text{TMT}(X, Z))$ twice since otherwise γ' would have a cycle. Since the number of triplets is finite, eventually, we must obtain a path γ' joining z_i to a point from X and with no edges from $\alpha(\text{TMT}(X, Z))$.

Now, for each $z_i \in Z \setminus X$, we consider the resulting path γ' joining z_i to a point $z_j \in X$, and we assume that $\gamma' \cap X = \{z_j\}$, as otherwise γ' can be shortened.

By the triangle inequality, we obtain $d^Z(z_i, z_j) \leq \sum_{(z_k, z_l) \in \gamma'} d^Z(z_k, z_l)$. Now, γ' lies in a connected component from $\text{VR}_{\eta_f}(Z)$, a path with maximum length c_f . Also, the lengths of the edges from γ' injectively correspond to lengths of edges from $\alpha(\text{TMT}(Z) \setminus \text{TMT}(X, Z))$. \square

Intuitively, the upper bound from Proposition 5.5 is computed by adding the η_f largest quantities along the right infinity line from $D(f)$.

6. Methodology and Applications

In this section, we apply the novel concepts introduced in this paper to two different datasets: the housing dataset and the dry beans dataset. The housing dataset is a standard dataset in machine learning and statistics, which contains various attributes related to housing prices and features. In contrast, the dry beans dataset encompasses morphological characteristics of different dry bean varieties, serving as an example from agricultural research. Both of them are tabular datasets, and their features are real-valued.

For both datasets, our approach involved training a multilayer perceptron (MLP) using a subset of the dataset and evaluating its performance on the remaining set as a test set to assess the generalization ability of the MLP. Then, we do a qualitative study based on the differences between the matched intervals and the size of the unmatched intervals (cokernel). This gives us an idea of how well each of the classes is represented by the subset as well as the shape of the dataset as a whole.

These experiments aim to show the robustness of the training process with respect to the training dataset, testing and highlighting the potential limitations of model performance evaluation when considering the dataset as a whole versus a subset.

6.1. Housing dataset

The Housing dataset² \mathcal{H} is composed of 20640 real-valued 8-dimensional samples for regression. In our case, we transformed it into a classification problem by discretizing the target values into three classes by intervals and normalizing the values of the features between 0 and 1. As a first example, we chose a random subset $X^{\mathcal{H}}$ of size 1000 and an MLP with $256 \times 128 \times 64$ ReLu hidden layers and a final output layer with Softmax activation function, that was trained for 1000 epochs using Adam training algorithm with a learning rate 0.001. We repeated the training 10 times, and the highest accuracy values we reached were 0.71 on the test set and 0.72 on the training set. For a more thorough study of the accuracy by classes for one of the iterations, see Figure 7. The confusion matrix shows that the class 2 has less accuracy than the other classes. Later, we computed the matching diagram $D(f^{\mathcal{H}})$ (see Figure 8) for $f^{\mathcal{H}} : \text{PH}_0(X^{\mathcal{H}}) \rightarrow \text{PH}_0(\mathcal{H})$. Such a diagram is a plot

²https://scikit-learn.org/stable/modules/generated/sklearn.datasets.fetch_california_housing.html

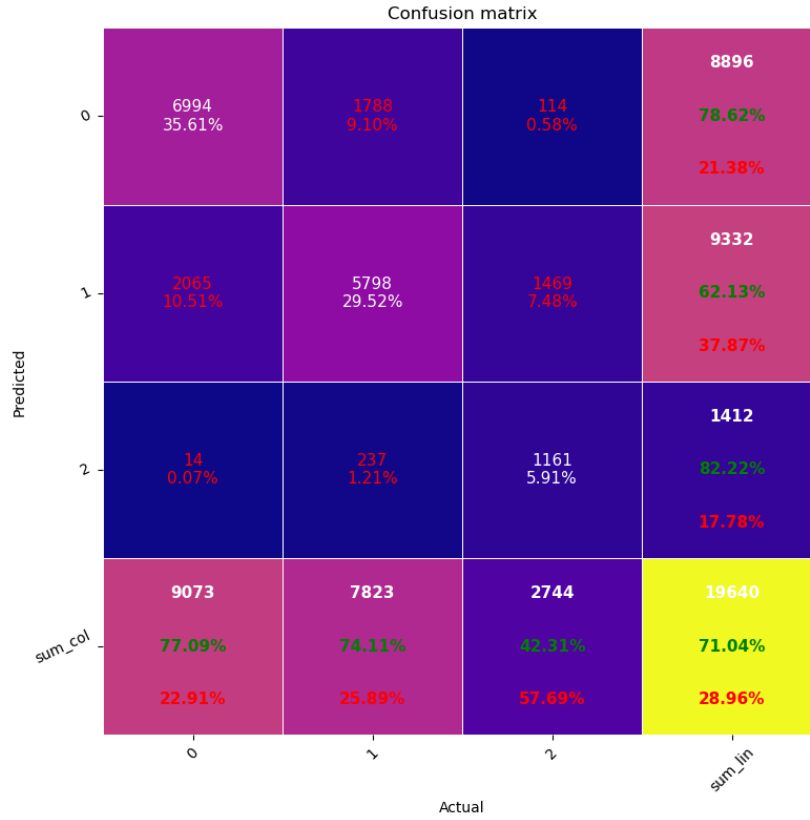


Figure 7: Housing dataset. Confusion matrix of the MLP trained on a random subset $X^{\mathcal{H}}$ of size 1000. We can see that class 2 shows lower performance.

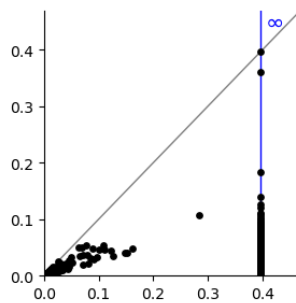


Figure 8: Housing dataset. Depiction of the matching diagram $D(f^{\mathcal{H}})$ associated to the subset $X^{\mathcal{H}}$ of size 1000 and the full dataset \mathcal{H} .

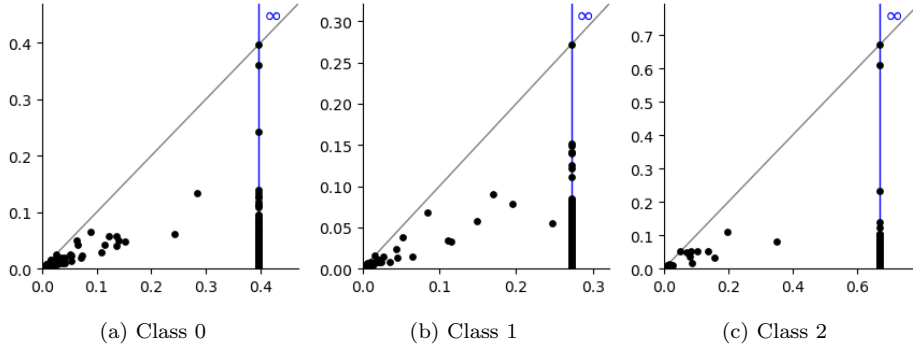


Figure 9: Housing dataset. Representation of the matching diagrams $D(f^{\mathcal{H}^{(i)}})$ for $i \in [3]$.

of 2-dimensional points whose coordinates are the endpoints of the matched intervals together with a representation of the cokernel of $f^{\mathcal{H}}$, which is plotted on a vertical line on the right side. The representativeness of \mathcal{H} through $X^{\mathcal{H}}$ is said to be “good” if points of $D(f^{\mathcal{H}})_o$ get close to the diagonal and cokernel points (i.e., points of $D(f^{\mathcal{H}})_\infty$) are close to $(\infty, 0)$. In Figure 8, we can see that most of the points of $D(f^{\mathcal{H}}) = D(f^{\mathcal{H}})_o \sqcup D(f^{\mathcal{H}})_\infty$ are concentrated at the origin $(0, 0)$ (meaning that matched intervals are small) and at the point $(\infty, 0)$ (meaning that unmatched intervals are small). Nevertheless, one matched interval difference reaches almost 0.3, and one unmatched interval (i.e., an interval in the cokernel of $f^{\mathcal{H}}$) has a length between 0.3 and 0.4. We can then expect some distortion of the original shape of the dataset with respect to the shape of the subset. In Figure 9, we provide the matching diagrams for each class. We denote by $D(f^{\mathcal{H}^{(i)}})$ the matching diagram corresponding to the restriction to the points of $X^{\mathcal{H}}$ and \mathcal{H} of the class i . As we can see, for class 2, the points of $D(f^{\mathcal{H}^{(2)}})_o$ tend to disperse to the right and far from the diagonal, which means bigger differences between the matched intervals; and one point of $D(f^{\mathcal{H}^{(2)}})_\infty$ (vertical line on the right) appear far from the x -axis. In particular, a point appears at y -value 0.6 much higher than any other point in any other class. Nevertheless, for class 0, the points of $D(f^{\mathcal{H}^{(2)}})_o$ are more concentrated on the origin. This agrees with what we obtained in the confusion matrix of the trained MLP, represented in Figure 7.

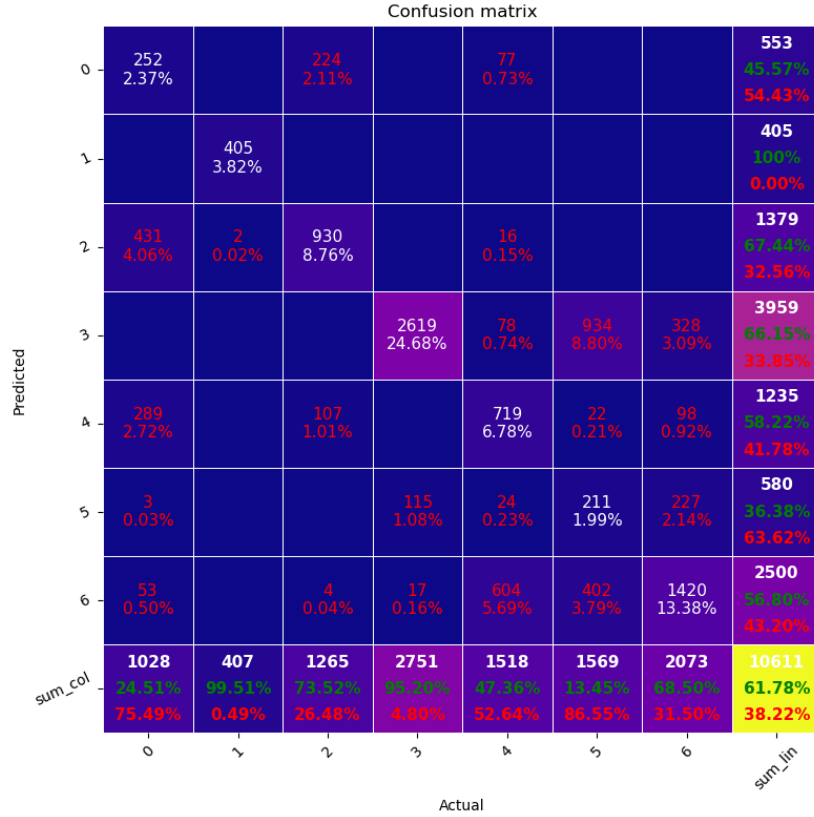


Figure 10: Beans dataset. Confusion matrix of the MLP trained on a random subset $X^B \subset \mathcal{B}$ of size 3000 evaluated on the test set. We can see that the class with the lowest performance is class 5, and the one with the highest performance is class 1.

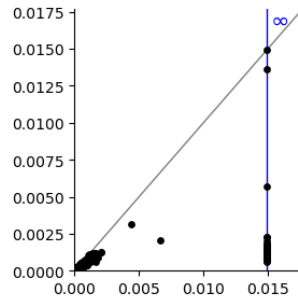


Figure 11: Beans dataset. Depiction of the matching diagram $D(f^B)$ between the random subset X^B and the full dataset \mathcal{B} .

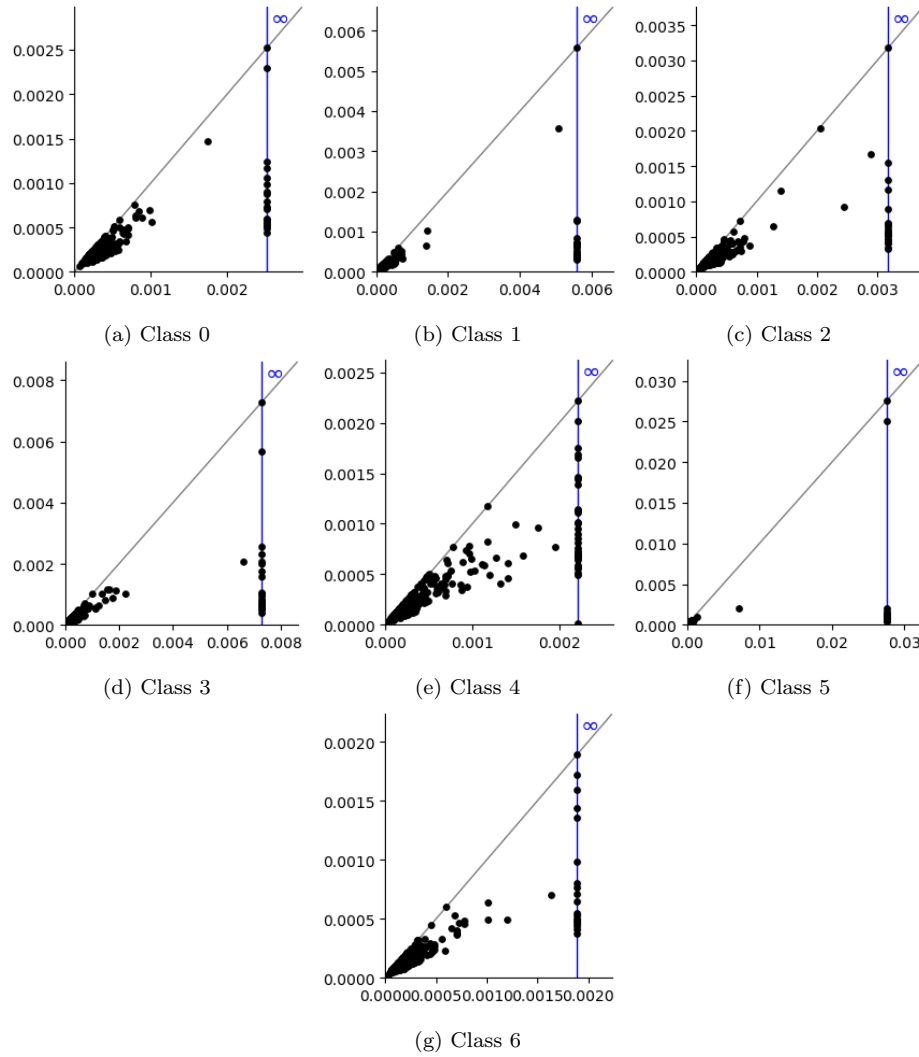


Figure 12: Beans dataset. Depiction of the matching diagram $D(f^{B^{(i)}})$ for $i \in \llbracket 7 \rrbracket$ corresponding to the restriction to the points of X^B and B belonging to the class i .

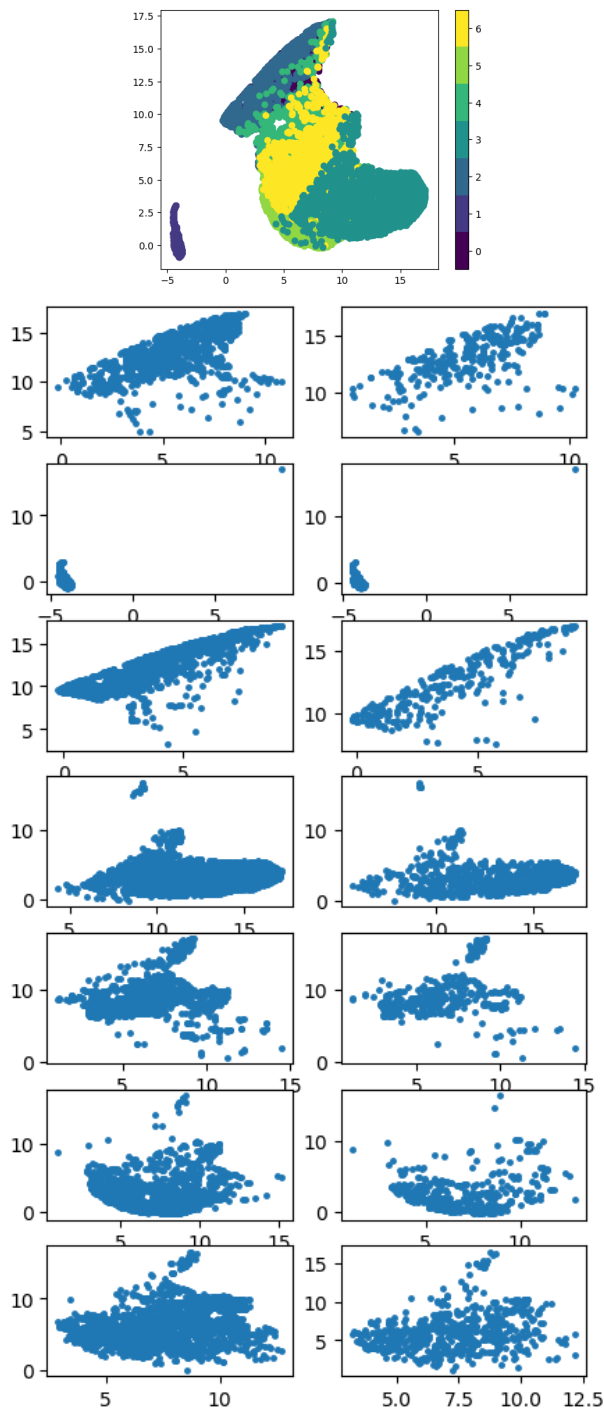


Figure 13: On the top, we can see the UMAP embedding of the dataset coloured by classes. Then, from top to bottom, the embeddings for the different classes are shown together with their subset.

6.2. Dry beans dataset

The dry beans dataset³ \mathcal{B} is composed of 13611 real-valued 16-dimensional samples obtained from measures taken from high-resolution images of 7 different types of grains.

In this experiment, we first chose a random subset $X^{\mathcal{B}}$ of size 3000, leaving the remaining set as a test set, and trained an MLP with $1024 \times 256 \times 128 \times 64$ ReLu hidden layers and a final output layer with Softmax activation function, which was trained for 1000 epochs using Adam training algorithm with learning rate 0.001. We repeated the training 10 times, and the highest accuracy value we reached was 0.63 on the test and training set. Figure 10 shows the confusion matrix on the test set for one of the iterations. There, we can see the accuracy for each of the classes. In this case, we can find that the class with the lowest performance is class 5, and the one with the highest performance is class 1. If we check the proportion of each class on the dataset, we appreciate that class 1 is the less represented and the one with the best performance, which seems contradictory. In Figure 11, $D(f^{\mathcal{B}})$ shows that, in general, intervals of $B(\text{PH}_0(X^{\mathcal{B}}))$ and $B(\text{PH}_0(\mathcal{B}))$ are well matched. In Figure 12, we can see that all the classes display similar matching diagrams and that points of $D(f^{\mathcal{B}(i)})_o$ for $i \in \llbracket 6 \rrbracket$ concentrate on the origin. Let us remark that the order of magnitude for the x -axis is 10^{-3} or lower for all classes except for class 5. Also, we can see higher values for this class on the y -axis and a point in the cokernel $D(f^{\mathcal{B}(5)})_{\infty}$ representing an unmatched interval of length close to 0.025. This explains the poor performance of the trained MLP regarding class 5. On the contrary, we can see that the cokernel of class 1, $D(f^{\mathcal{B}(1)})_{\infty}$, presents all points close to the horizontal axis which explains the good performance of the trained MLP regarding class 1.

Finally, we computed a 2-dimensional embedding of the dataset \mathcal{B} (see Figure 13) using the UMAP algorithm [10] to check the intuition provided by $D(f^{\mathcal{B}})$. The embedding shows how class 1 is isolated by the embedding, making it easier to classify by the model. We can see how the class 5 shape seems to be badly represented and mixed with other classes, supporting the findings given by the matching diagram $D(f^{\mathcal{B}})$.

³<https://archive.ics.uci.edu/dataset/602/dry+bean+dataset>

7. Conclusion and future works

In this paper, we have introduced a novel definition of data quality based on topological features obtained from 0-dimensional persistence modules, induced block functions and persistence matchings to measure the quality of a training subset relative to the entire input dataset. Theoretical results support that the proposed definition is well-founded. The experimentation reveals that the topological data quality information is coherent with related tools to visualize/inspect datasets and demonstrates that it is a valuable measure, providing insights into why a chosen training subset might lead to poor performance.

There are different research lines for future work. An interesting direction is to adapt our method to be robust to outliers and to optimize our code for large datasets. While our method is polynomial in theory, persistent homology is linear in practice, and we believe our method can achieve linear performance in practice too. Specifically, a future direction is to adapt the work from [12] to compute steps 1 and 2 directly, which is likely more efficient and parallelisable since the current computational bottleneck of our implementation is in computing the minimum spanning tree in Step 1. Additionally, we have observed that the distance metric used to compute persistent homology should be related to the architecture chosen. For example, if we use Euclidean distance, it makes sense to use perceptions. If using the Structural Similarity Index Measure (SSIM) or the Fréchet Inception Distance (FID), a convolutional neural network (CNN) should be used as the architecture. Moreover, in our future work, we will explore scenarios where X is not a subset of Z and topological features of dimensions higher than 0. For instance, using 1-dimensional persistence matchings can help in cases where 0-dimensional topological features are not decisive.

Code Availability

The source code for the examples and experiments described in this paper is available on the GitHub repository <https://github.com/Cimagroup/tdqual>.

Acknowledgments

This work received funding from the Horizon Europe research and innovation program under grant agreement no. 101070028-2 REXASI-PRO “RE-

liable & eXplainable Swarm Intelligence for People with Reduced mObility” (call HORIZON-CL4-2021-HUMAN-01-01), and from MCIN/AEI/10.13039/501100011033 and the European Union NextGenerationEU/PRTR, under the national project TED2021-129438B-I00 “Computational Topology for energy saving and optimization of deep learning methods to achieve Green Artificial Intelligence solutions”.

References

- [1] U. Bauer and M. Lesnick. Induced matchings and the algebraic stability of persistence barcodes. *Journal of Computational Geometry*, 6:162–191, 3 2015.
- [2] E. M. Bender, T. Gebru, A. McMillan-Major, and S. Shmitchell. On the dangers of stochastic parrots: Can language models be too big? In *Proc of the 2021 ACM Conf on Fairness, Accountability, and Transparency*, page 610–623, 2021. ISBN 9781450383097. doi: 10.1145/3442188.3445922.
- [3] G. Carlsson and M.I Vejdemo-Johansson. *Topological Data Analysis with Applications*. Cambridge University Press, 2021. doi: 10.1017/9781108975704.
- [4] F. Chazal, V. de Silva, M. Glisse, and S. Y. Oudot. *The Structure and Stability of Persistence Modules*. Springer Briefs in Mathematics. Springer, 2016. ISBN 978-3-319-42543-6. doi: 10.1007/978-3-319-42545-0.
- [5] D. Cohen-Steiner, H. Edelsbrunner, J. Harer, and D. Morozov. *Persistent Homology for Kernels, Images, and Cokernels*. Proc. of the 2009 Annual ACM-SIAM Symposium on Discrete Algorithms (SODA).
- [6] W. Crawley-Boevey. Decomposition of pointwise finite-dimensional persistence modules. *Journal of Algebra and Its Applications*, 14(5), 2015.
- [7] H. Edelsbrunner and J. Harer. *Computational Topology: An Introduction*. Applied Mathematics. American Mathematical Society, 2010. ISBN 9780821849255.

- [8] R. Gonzalez-Diaz, M. Soriano-Trigueros, and A. Torras-Casas. Partial matchings induced by morphisms between persistence modules. *Computational Geometry*, 112:101985, 2023. ISSN 0925-7721. doi: 10.1016/j.comgeo.2023.101985.
- [9] E. Jacquard, V. Nanda, and U. Tillmann. The space of barcode bases for persistence modules. *Journal of Applied and Computational Topology*, 7:1–30, 2023. doi: 10.1007/s41468-022-00094-6.
- [10] L. McInnes, J. Healy, and J. Melville. Umap: Uniform manifold approximation and projection for dimension reduction, 2020. URL <https://arxiv.org/abs/1802.03426>.
- [11] S. Y. Oudot. *Persistence Theory: From Quiver Representations to Data Analysis*. Number volume 209 in Mathematical Surveys and Monographs. AMS, 2015. ISBN 9781470425456.
- [12] D. Smirnov and D. Morozov. Triplet merge trees. In H. Carr, I. Fujishiro, F. Sadlo, and S. Takahashi, editors, *Topological Methods in Data Analysis and Visualization V*, pages 19–36, Cham, 2020. Springer International Publishing.

Appendix A. Proof of Proposition 2.10

The aim of this appendix is to show the stability of $\text{im}(f)$, $\text{ker}(f)$ and $\text{coker}(f)$. The original result of this fact can be found in [5]. However, the Stability Theorem shown in [5] is formulated in terms of pairs of continuous functions $f, f' : L \rightarrow \mathbb{R}$ given an underlying topological space L and such that $\|f - f'\| < \varepsilon$. Thus, we would need to adapt the existing Stability Theorem to the Gromov-Hausdorff distance and the case of persistence morphisms induced by an inclusion. Instead, we choose to prove such stability by a simple argument, which aids in making the article self-contained.

To start, we recall the definition of interleaving distance between two persistence modules. Given a persistence module V with structure maps ρ^V and given $\varepsilon \geq 0$, we denote by $V(\varepsilon)$ the persistence module such that $V(\varepsilon)_r = V_{r+\varepsilon}$ for all $r \in \mathbb{R}$ and with structure maps $\rho_{rs}^{V(\varepsilon)} = \rho_{r+\varepsilon, s+\varepsilon}^V$ for all $r \leq s$.

We denote by ρ_ε^V the persistence morphism $\rho_\varepsilon^V : V \rightarrow V(\varepsilon)$ given by $(\rho_\varepsilon^V)_r = \rho_{r+\varepsilon}^V$ for all $r \geq 0$. Also, given a persistence morphism $f : V \rightarrow U$,

we denote by f_ε the persistence morphism $f_\varepsilon : V(\varepsilon) \rightarrow U(\varepsilon)$ such that $(f_\varepsilon)_r = f_{r+\varepsilon}$ for all $r \in \mathbb{R}$.

We say that two persistence modules V and U are ε -interleaved if there exist persistence morphisms, $\phi : V \rightarrow U(\varepsilon)$ and $\psi : U \rightarrow V(\varepsilon)$, such that $\psi_\varepsilon \circ \phi = \rho_{2\varepsilon}^V$ and also $\phi_\varepsilon \circ \psi = \rho_{2\varepsilon}^U$. The *interleaving distance* between V and U is defined as follows

$$d_I(V, U) = \inf \{ \varepsilon \geq 0 \mid V \text{ and } U \text{ are } \varepsilon\text{-interleaved} \}.$$

The following result is adapted from Proposition 7.8 from [11].

Proposition Appendix A.1. *Let X and X' be two finite metric spaces. Let $V = \text{PH}_0(X)$ and $V' = \text{PH}_0(X')$. Then, $d_I(V, V') \leq 2d_{GH}(X, X')$.*

Now we present another result known as the *Isometry Theorem* which is Theorem 3.5 from [1]. A persistence module V is said to be *pointwise finite dimensional* (p.f.d) whenever $\dim(V_r) < \infty$ for all $r \in \mathbb{R}$.

Proposition Appendix A.2. *Let V and V' be two p.f.d. persistence modules. Then, $d_B(\text{B}(V), \text{B}(V')) = d_I(V, V')$.*

In this work, all persistence modules are p.f.d. since these are either of the form $\text{PH}_0(Z)$ for a finite metric space Z or are $\text{im}(f)$, $\text{ker}(f)$ or $\text{coker}(f)$ for a persistence morphism f between p.f.d. persistence modules.

Next, we define the interleaving distance between persistence morphisms. Let $f : V \rightarrow U$ and $f' : V' \rightarrow U'$ be a pair of persistence morphisms. We say that f and f' are ε -interleaved if there exists four persistence morphisms, $\phi : V \rightarrow V'(\varepsilon)$, $\phi' : V' \rightarrow V(\varepsilon)$, $\psi : U \rightarrow U'(\varepsilon)$ and $\psi' : U' \rightarrow U(\varepsilon)$ such that:

- $\phi'_\varepsilon \circ \phi = \rho_{2\varepsilon}^V$, $\phi_\varepsilon \circ \phi' = \rho_{2\varepsilon}^{V'}$,
- $\psi'_\varepsilon \circ \psi = \rho_{2\varepsilon}^U$, $\psi_\varepsilon \circ \psi' = \rho_{2\varepsilon}^{U'}$,
- $\psi \circ f = f'_\varepsilon \circ \phi$ and $\psi' \circ f' = f_\varepsilon \circ \phi'$.

Then the interleaving distance between f and f' is:

$$d_I(f, f') = \inf \{ \varepsilon \geq 0 \mid f \text{ and } f' \text{ are } \varepsilon\text{-interleaved} \}.$$

Now, assuming that f and f' are ε -interleaved, we have the following result.

Proposition Appendix A.3. *Given $\varepsilon = d_I(f, f')$, then*

$$\begin{aligned} d_I(\text{im}(f), \text{im}(f')) &\leq \varepsilon, \\ d_I(\ker(f), \ker(f')) &\leq \varepsilon, \text{ and} \\ d_I(\text{coker}(f), \text{coker}(f')) &\leq \varepsilon. \end{aligned}$$

PROOF. Let us see the first inequality. The commutativity relation $\psi \circ f = f'_\varepsilon \circ \phi$ implies $\psi(\text{im}(f)) \subseteq \text{im}(f')(\varepsilon)$. Also, $\psi' \circ f' = f_\varepsilon \circ \phi'$ implies $\psi'(\text{im}(f')) \subseteq \text{im}(f)(\varepsilon)$. Hence, ψ and ψ' restrict to an ε -interleaving between $\text{im}(f)$ and $\text{im}(f')$.

Next, we consider the following commutative diagram

$$\begin{array}{ccccc} \text{im}(f) & \hookrightarrow & U & \twoheadrightarrow & \text{coker}(f) \\ \downarrow \psi|_{\text{im}(f)} & & \downarrow \psi & & \downarrow \bar{\psi} \\ \text{im}(f')(\varepsilon) & \hookrightarrow & U'(\varepsilon) & \twoheadrightarrow & \text{coker}(f')(\varepsilon) \end{array}$$

where the arrow $\bar{\psi}$ is such that it commutes in the diagram. By a similar commutativity argument, one can define $\bar{\psi}' : \text{coker}(f') \rightarrow \text{coker}(f)(\varepsilon)$. Also, since $\psi'_\varepsilon \circ \psi = \rho_{2\varepsilon}^U$, it follows that $\bar{\psi}'_\varepsilon \circ \bar{\psi} = \rho_{2\varepsilon}^{\text{coker}(f)}$. Similarly, we also have $\bar{\psi}^\varepsilon \circ \bar{\psi}' = \rho_{2\varepsilon}^{\text{coker}(f')}$. Hence, $\text{coker}(f)$ and $\text{coker}(f')$ are ε -interleaved.

Finally, by equalities $\psi \circ f = f'_\varepsilon \circ \phi$ and $\psi' \circ f' = f_\varepsilon \circ \phi'$ we have inclusions $\phi(\ker(f)) \subseteq \ker(f')(\varepsilon)$ and $\phi'(\ker(f')) \subseteq \ker(f)(\varepsilon)$. Altogether, ϕ and ϕ' restrict to an ε -interleaving between $\ker(f)$ and $\ker(f')$. \square

Next, we adapt Proposition Appendix A.1 to persistence morphisms induced by inclusions. In particular, the following result works for 0-dimensional persistent homology.

Proposition Appendix A.4. *Let $X \subseteq Z$ and $X' \subseteq Z'$ be finite metric spaces. Let $V = \text{PH}_0(X)$, $V' = \text{PH}_0(X')$, $U = \text{PH}_0(Z)$ and $U' = \text{PH}_0(Z')$. Let $f : V \rightarrow U$ and $f' : V' \rightarrow U'$ be the persistence morphisms induced by the inclusions. Then, $d_I(f, f') \leq 2d_{GH}((X, Z), (X', Z'))$.*

PROOF. Let $\varepsilon = d_{GH}((X, Z), (X', Z'))$. There exists a metric space M together with a pair of isometries $\gamma_Z : Z \hookrightarrow M$ and $\gamma_{Z'} : Z' \hookrightarrow M$ such that $d_H^M(\gamma_Z(Z), \gamma_{Z'}(Z')) \leq \varepsilon$ and $d_H^M(\gamma_Z(X), \gamma_{Z'}(X')) \leq \varepsilon$. Thus, we consider an assignment $\alpha^X : X \rightarrow X'$ sending a point $x \in X$ to $\alpha^X(x) \in X'$

such that $d^M(\gamma_Z(x), \gamma_{Z'}(\alpha^X(x))) \leq \varepsilon$. Then, we extend α^X to an assignment $\alpha^Z : Z \rightarrow Z'$ such that $\alpha^Z|_X = \alpha^X$ and that $d^M(\gamma_Z(z), \gamma_{Z'}(\alpha^Z(z))) \leq \varepsilon$ for all $z \in Z$.

Similarly, we define an assignment $\alpha^{Z'} : Z' \rightarrow Z$ such that $d^M(\gamma_Z(\alpha^{Z'}(z')), \gamma_{Z'}(z')) \leq \varepsilon$ for all $z' \in Z'$ and $\alpha^{Z'}(X') \subseteq X$, so we define $\alpha^{X'} = \alpha^{Z'}|_{X'}$.

Such assignments determine well-defined morphisms of graphs, $\alpha^Z : \text{VR}_r(Z) \rightarrow \text{VR}_{r+2\varepsilon}(Z')$ and $\alpha^{Z'} : \text{VR}_r(Z') \rightarrow \text{VR}_{r+2\varepsilon}(Z)$, for all $r \geq 0$, where, for example, given an edge $[u, v] \in \text{VR}_r(Z)$ we have $\alpha^Z([u, v]) = [\alpha^Z(u), \alpha^Z(v)] \in \text{VR}_{r+2\varepsilon}(Z')$; here notice that we have used that γ_Z is an isometry together with the triangle inequality on d^M :

$$\begin{aligned} d^{Z'}(\alpha^Z(u), \alpha^Z(v)) &= d^M(\gamma_{Z'}(\alpha^Z(u)), \gamma_{Z'}(\alpha^Z(v))) \\ &\leq d^M(\gamma_{Z'}(\alpha^Z(u)), \gamma_Z(u)) + d^M(\gamma_Z(u), \gamma_Z(v)) + d^M(\gamma_Z(v), \gamma_{Z'}(\alpha^Z(v))) \\ &\leq \varepsilon + r + \varepsilon = r + 2\varepsilon. \end{aligned}$$

Further, notice that α^X and $\alpha^{X'}$ are such that $\alpha^X(\text{VR}_r(X)) \subseteq \text{VR}_{r+2\varepsilon}(X')$ and $\alpha^{X'}(\text{VR}_r(X')) \subseteq \text{VR}_{r+2\varepsilon}(X)$.

Altogether, by construction, α^X and α^Z induce persistence morphisms, $\phi^X : V \rightarrow V'(2\varepsilon)$ and $\psi^Z : U \rightarrow U'(2\varepsilon)$, such that $\psi^Z \circ f = f'_{2\varepsilon} \circ \phi^X$. Similarly, $\alpha^{X'}$ and $\alpha^{Z'}$ induce persistence morphisms, $\phi^{X'} : V' \rightarrow V(2\varepsilon)$ and $\psi^{Z'} : U' \rightarrow U(2\varepsilon)$, such that $\psi^{Z'} \circ f' = f_{2\varepsilon} \circ \phi^{X'}$.

Also by construction of α^Z and $\alpha^{Z'}$, we have the other equalities that make that f and f' are 2ε -interleaved, concluding that $d_I(f, f') \leq 2\varepsilon$. \square

Now we are ready to prove Proposition 2.10.

PROOF (OF PROPOSITION 2.10). First, since $\varepsilon = d_{GH}((X, Z), (X', Z'))$ then, by Proposition Appendix A.4, we have that $d_I(f, f') \leq 2\varepsilon$. Now, we obtain the inequalities in the statement of the proposition directly by applying Proposition Appendix A.3. \square

Appendix B. Proof of Theorem 4.6

As the section indicates, here our aim is to prove Theorem 4.6. To start, we consider two sub-multisets from $D(f)$. We denote by $D(f)_o$ the sub-multiset of $D(f)$ given by the pairs $(a, b) \in D(f)$ with $a < \infty$ and with multiplicity $m^{D(f)}((a, b))$. On the other hand, we denote by $D(f)_\infty$ the multiset of pairs $(\infty, b) \in D(f)$ with multiplicity $m^{D(f)}((\infty, b))$. In particular,

one has the disjoint union $D(f) = D(f)_o \sqcup D(f)_\infty$. We prove Theorem 4.6 based on the following two results.

Proposition Appendix B.1. *Given $\varepsilon = d_{GH}((X, Z), (X', Z'))$, there exists a partial matching*

$$\sigma^\infty : \text{Rep } D(f)_\infty \dashrightarrow \text{Rep } D(f')_\infty$$

sending $((\infty, b), i) \in \text{coim}(\sigma^\infty)$ to an element $((\infty, b'), j)$ with $|b - b'| < 2\varepsilon$ and such that, given $((\infty, b), i) \in \text{Rep } D(f)_\infty \setminus \text{coim } \sigma^\infty$ then $b < 2\varepsilon$ or given $((\infty, b'), i) \in \text{Rep } D(f')_\infty \setminus \text{im } \sigma^\infty$ then $b' < 2\varepsilon$.

PROOF. To start, we recall that there are a couple of bijections $\mu : \text{Rep } D(f)_\infty \rightarrow \text{Rep } B(\text{coker}(f))$ (given by sending $((\infty, b), i) \in \text{Rep } D(f)_\infty$ to $([0, b], j) \in \text{Rep } B(\text{coker}(f))$) and $\mu' : \text{Rep } D(f')_\infty \rightarrow \text{Rep } B(\text{coker}(f'))$. Now, by Propositions Appendix A.2 and Appendix A.3 we have $d_B(\text{coker}(f), \text{coker}(f')) < 2\varepsilon$. Consequently, there exists a partial matching $\sigma^{\text{coker}} : \text{Rep } B(\text{coker}(f)) \dashrightarrow \text{Rep } B(\text{coker}(f'))$ that sends $([0, b], i)$ to $([0, b'], j)$ with $|b - b'| < 2\varepsilon$ or, given $([0, b], i) \in \text{Rep } B(\text{coker}(f))$ unmatched, then $b < 2\varepsilon$ and given $([0, b'], i) \in \text{Rep } B(\text{coker}(f'))$ unmatched then $b' < 2\varepsilon$. \square

The second result that we need requires more work, and we delay the proof for later.

Proposition Appendix B.2. *Given $\varepsilon = d_{GH}((X, Z), (X', Z'))$, there exists a partial matching*

$$\sigma^o : \text{Rep } D(f)_o \dashrightarrow \text{Rep } D(f')_o$$

such that given $((a, b), i) \in \text{coim}(\sigma^o)$ we have $\sigma^o((a, b), i) = ((a', b'), j)$ with $|a - a'| < 2\varepsilon$ and $|b - b'| < 2\varepsilon$ or, given $((a, b), i) \in \text{Rep } D(f)_o \setminus \text{coim}(\sigma^o)$ then $b \leq a < 2\varepsilon$ or given $((a', b'), j) \in \text{Rep } D(f')_o \setminus \text{im}(\sigma^o)$ then $b' \leq a' < 2\varepsilon$.

Now, we are ready to prove Theorem 4.6.

PROOF (OF THEOREM 4.6). We consider a partial matching $\sigma^{D(f)} : D(f) \dashrightarrow D(f')$ that is the combination of σ^∞ and σ^o produced in Propositions Appendix B.1 and Appendix B.2. Since $D(f)$ is the disjoint union $D(f) = D(f)_o \sqcup D(f)_\infty$ then, by construction of σ^∞ and σ^o , the partial matching $\sigma^{D(f)}$ fulfills the requirements given in the statement of Theorem 4.6, concluding the proof. \square

The rest of this section is devoted to prove Proposition Appendix B.2. For this, we consider fixed finite metric spaces Z and Z' and subsets $X \subseteq Z$ and $X' \subseteq Z'$ such that $\varepsilon = d_{GH}((X, Z), (X', Z'))$ and persistence morphisms $f : V \rightarrow U$ and $f' : V' \rightarrow U'$ induced by the inclusions. Recall the assignments α^Z and $\alpha^{Z'}$ from Proposition Appendix A.3. We pay close attention to their restrictions $\alpha^X = \alpha^Z|_X : X \rightarrow X'$ and $\alpha^{X'} = \alpha^{Z'}|_{X'} : X' \rightarrow X$ and use them to define a subset $Y \subseteq X \times X'$ given by pairs $(x, x') \in X \times X'$ such that either $\alpha^X(x) = x'$ or $\alpha^{X'}(x') = x$. Fixed $\delta > 0$, we denote by Y^δ the metric space with set Y and metric d^{Y^δ} where, given $(x, x'), (y, y') \in Y^\delta$ we have

$$d^{Y^\delta}((x, x'), (y, y')) = \begin{cases} 0 & \text{if } (x, x') = (y, y') \\ \delta + d^X(x, y) & \text{otherwise} \end{cases}$$

We can also define $Y^{\delta'}$ with distance $d^{Y^{\delta'}}$ where, given $(x, x'), (y, y') \in Y$, we have

$$d^{Y^{\delta'}}((x, x'), (y, y')) = \begin{cases} 0 & \text{if } (x, x') = (y, y') \\ \delta + d^{X'}(x', y') & \text{otherwise} \end{cases}$$

There are nonexpansive maps $\pi : Y^\delta \rightarrow X$ and $\pi' : Y^{\delta'} \rightarrow X'$ given by $\pi((x, x')) = x$ and $\pi'((x, x')) = x'$ for all $(x, x') \in Y$. Now, we define the persistence modules $W = \text{PH}_0(Y^\delta)$ and $W' = \text{PH}_0(Y^{\delta'})$ and consider the persistence morphisms $h : W \rightarrow V$ and $h' : W' \rightarrow V'$ induced by π and π' , respectively. We write $f^\delta = f \circ h : W \rightarrow U$ and $f^{\delta'} = f' \circ h' : W' \rightarrow U'$.

Proposition Appendix B.3. $d_I(f^\delta, f^{\delta'}) \leq 2\varepsilon$ for any $\delta > 0$.

PROOF. Let us see that f^δ and $f^{\delta'}$ are 2ε -interleaved. First, we can define two morphisms of graphs, for all $r \geq 0$, $\alpha^{Y^\delta} : \text{VR}_r(Y^\delta) \rightarrow \text{VR}_{r+2\varepsilon}(Y^{\delta'})$ and $\alpha^{Y^{\delta'}} : \text{VR}_r(Y^{\delta'}) \rightarrow \text{VR}_{r+2\varepsilon}(Y^\delta)$ by using the identity on Y . To show that α^{Y^δ} is well-defined, consider different pairs $(x, x'), (y, y') \in Y$ such that $d^Z(x, y) = r$, there is an inequality

$$\begin{aligned} d^{Y^{\delta'}}((x, x'), (y, y')) - \delta &= d^{X'}(x', y') = d^M(\gamma_{Z'}(x'), \gamma_{Z'}(y')) \\ &\leq d^M(\gamma_{Z'}(x'), \gamma_Z(x)) + d^M(\gamma_Z(x), \gamma_Z(y)) + d^M(\gamma_Z(y), \gamma_{Z'}(y')) \leq (r - \delta) + 2\varepsilon. \end{aligned}$$

Similarly, $\alpha^{Y^{\delta'}}$ is well-defined. In turn, these induce a pair of persistence morphisms $\phi^Y : W \rightarrow W'(2\varepsilon)$ and $\phi^{Y'} : W' \rightarrow W(2\varepsilon)$ such that $\phi_{2\varepsilon}^{Y'} \circ \phi^Y = \rho_{4\varepsilon}^W$ and $\phi_{2\varepsilon}^Y \circ \phi^{Y'} = \rho_{4\varepsilon}^{W'}$.

On the other hand, there is a commutative relation $\phi^X \circ h = h'_{2\varepsilon} \circ \phi^Y$ which we need to prove. First, notice that, for any $(x, x') \in Y$ we have that $[\alpha^X(x), x']$ is an edge in $\text{VR}_{2\varepsilon}(X')$, and, in particular, given $r \geq 0$, the class $[(x, x')] \in W_r$ is such that there is an equality in $V_{r+2\varepsilon}$:

$$(\phi^X)_{r+2\varepsilon} \circ h_r([(x, x')]) = [\alpha^X(x)] = [x'] = (h'_{2\varepsilon})_r \circ \phi_r^Y([(x, x')]).$$

Since $\{[(x, x')] \mid (x, x') \in Y\}$ is a set of generators for W_r , we can conclude that $(\phi^X \circ h)_r = (h'_{2\varepsilon} \circ \phi^Y)_r$. By the same principle, $\phi^{X'} \circ h' = h_{2\varepsilon} \circ \phi^{Y'}$. Using these relations, and since, by Proposition Appendix A.4, we have $f'_{2\varepsilon} \circ \phi^X = \psi^Z \circ f$ and $f_{2\varepsilon} \circ \phi^{X'} = \psi^{Z'} \circ f'$ we can see that:

$$f_{2\varepsilon}^{\delta'} \circ \phi^Y = f'_{2\varepsilon} \circ h'_{2\varepsilon} \circ \phi^Y = f'_{2\varepsilon} \circ \phi^X \circ h = \psi^Z \circ f^\delta$$

as well as

$$f_{2\varepsilon}^{\delta'} \circ \phi^{Y'} = f_{2\varepsilon} \circ h_{2\varepsilon} \circ \phi^{Y'} = f_{2\varepsilon} \circ \phi^{X'} \circ h' = \psi^{Z'} \circ f^{\delta'}.$$

This completes the proof since we know by Proposition Appendix A.4 that $\psi_{2\varepsilon}^{Z'} \circ \psi^Z = \rho_{4\varepsilon}^U$ and also $\psi_{2\varepsilon}^Z \circ \psi^{Z'} = \rho_{4\varepsilon}^{U'}$. \square

The following result shows that all intervals from $\text{B}(\ker(f^\delta))$ have length greater or equal to δ .

Lemma Appendix B.4. *All intervals from $\text{B}(\ker(f^\delta))$ are of the form $[b, a + \delta)$ with $0 < b \leq a$ or $[0, \delta)$. Besides, an interval $[b, a + \delta) \in \text{B}(\ker(f^\delta))$ with $0 < b \leq a$ has multiplicity $m^{f^\delta}([b, a + \delta)) = \mathcal{M}_f^0(a, b)$ and $m^{f^\delta}([0, \delta)) = \dim(\ker(h_0))$.*

PROOF. First, by definition of W , it follows that $\ker_b^\pm(W) = 0$ for $b < \delta$, while $\ker_\delta^+(W) = \ker(h_0)$. In addition, since $f_0^\delta = f_0 \circ h_0$ and $\ker(f_0) = 0$, it follows that $\ker(f_0^\delta) = \ker(h_0)$. Using this observation, together with Lemma 2.9 and commutativity of $\mathcal{M}_{f^\delta}^0$ with direct sums, there is an isomorphism

$$f^\delta \simeq \left(\bigoplus_{b>0} \bigoplus_{a \geq b} \bigoplus_{s \in \llbracket \mathcal{M}_{f^\delta}^0(a, b) \rrbracket} (\kappa_a \rightarrow \kappa_b) \right) \oplus \left(\bigoplus_{b>0} \bigoplus_{s \in \llbracket d_b^- \rrbracket} (0 \rightarrow \kappa_b) \right) \\ \oplus \left(\bigoplus_{s \in \llbracket d_\delta^+ \rrbracket} (\kappa_\delta \rightarrow 0) \right) \oplus (\kappa_\infty \rightarrow \kappa_\infty).$$

for $d_\delta^+ = \dim(\ker(h_0))$ and some integers $d_b^- \geq 0$ for all $b > 0$.

Now, we observe that by definition of W :

$$h_0(\ker_b^\pm(W)) = \begin{cases} 0 & \text{for } b \leq \delta, \\ \ker_{b-\delta}^\pm(V) & \text{for } \delta < b. \end{cases}$$

After these observations, using the partial matching formula we have

$$\mathcal{M}_{f^\delta}^0(a, b) = \begin{cases} 0 & \text{for } a \leq \delta, \\ \mathcal{M}_f^0(a - \delta, b) & \text{for } \delta < a. \end{cases}$$

In particular, this also implies that $N_{f^\delta}(b) = N_f(b)$ for all $b > 0$. Now, using our decomposition for f^δ , there is an isomorphism

$$\ker(f^\delta) \simeq \left(\bigoplus_{b>0} \bigoplus_{a \geq b} \bigoplus_{s \in \llbracket \mathcal{M}_f^0(a, b) \rrbracket} \kappa_b \rightarrow \kappa_{a+\delta} \right) \oplus \left(\bigoplus_{s \in \llbracket d_\delta^+ \rrbracket} \kappa_\delta \rightarrow 0 \right)$$

and so $B(\ker(f^\delta))$ is the multiset $(S^{f^\delta}, m^{f^\delta})$ given by

$$S^{f^\delta} = \{[b, a + \delta] \text{ such that } \mathcal{M}_f^0(a, b) \neq 0\} \cup \{[0, \delta]\}$$

and with multiplicities $m^{f^\delta}([b, a + \delta]) = \mathcal{M}_f^0(a, b)$ for $b > 0$ and $m^{f^\delta}([0, \delta]) = \dim(\ker(h_0))$. \square

The following result is why we are interested in f^δ and is the last ingredient we need to prove Proposition Appendix B.2.

Proposition Appendix B.5. *There exists an injection*

$$\sigma : \text{Rep } D(f)_o \hookrightarrow \text{Rep } B(\ker(f^\delta))$$

such that $((a, b), i) \in D(f)_o$ is sent to $([b, a + \delta], j) \in \text{Rep } B(\ker(f^\delta))$ and such that given $([c, d], l) \in B(\ker(f^\delta)) \setminus \text{im } \sigma$ then $c = 0$ and $d = \delta$.

There is also an analogous injection $\sigma' : \text{Rep } D(f')_o \hookrightarrow \text{Rep } B(\ker(f^{\delta'}))$.

PROOF. The result follows from Lemma Appendix B.4, recalling that $D(f)_o$ is the multiset given by pairs $(a, b) \in \mathbb{R} \times \mathbb{R}$ with multiplicities $m^{D(f)} = \mathcal{M}_f(a, b)$. \square

Finally, we are ready to provide the proof of Proposition Appendix B.2.

PROOF (OF PROPOSITION APPENDIX B.2). First, we fix $\delta > 2\varepsilon$. By Proposition Appendix B.3, $d_I(f^\delta, f^{\delta'}) \leq 2\varepsilon$. In particular, by Proposition Appendix A.3 we also have that $d_I(\ker(f^\delta), \ker(f^{\delta'})) \leq 2\varepsilon$ which in turn, by Proposition Appendix A.2, implies that $d_B(\mathbb{B}(\ker(f^\delta)), \mathbb{B}(\ker(f^{\delta'}))) \leq 2\varepsilon$. Thus, there exists a 2ε -partial matching $\sigma^{\ker} : \text{Rep } \mathbb{B}(\ker(f^\delta)) \dashrightarrow \mathbb{B}(\ker(f^{\delta'}))$. Besides, since all elements $([a, b], i) \in \text{Rep } \mathbb{B}(\ker(f^\delta))$ are such that $|a - b| \geq \delta > 2\varepsilon$ and all $([a', b'], j) \in \text{Rep } \mathbb{B}(\ker(f^{\delta'}))$ are such that $|a' - b'| \geq \delta > 2\varepsilon$, it follows that σ^{\ker} must be a bijection sending $([a, b], i) \in \text{Rep } \mathbb{B}(\ker(f^\delta))$ to $([a', b'], j) \in \text{Rep } \mathbb{B}(\ker(f^{\delta'}))$ with $|a - a'| < 2\varepsilon$ and $|b - b'| < 2\varepsilon$. Now, the claimed partial matching σ^o follows by the commutative square, where σ, σ' are from applying Proposition Appendix B.5 to f^δ and $f^{\delta'}$

$$\begin{array}{ccc} \text{Rep } D(f)_o & \xleftarrow{\sigma} & \text{Rep } \mathbb{B}(\ker(f^\delta)) \\ \downarrow \sigma^o & & \downarrow \sigma^{\ker} \\ \text{Rep } D(f')_o & \xleftarrow{\sigma'} & \text{Rep } \mathbb{B}(\ker(f^{\delta'})) \end{array}.$$

That is, σ^o is such that:

- If $((a, b), i) \in \text{Rep } D(f)_o \setminus \text{coim } \sigma^o$, then $\sigma^o((a, b), i) = ([b, a + \delta], j)$ and $\sigma^{\ker}([b, a + \delta], i') = ([0, \delta], k)$, which implies that $a = |(a + \delta) - \delta| < 2\varepsilon$.
- For $((a, b), i) \in \text{coim } \sigma^o$, then $\sigma^o((a, b), i) = ((a', b'), j) \in \text{Rep } D(f')_o$ such that $\sigma((a, b), i) = ([b, a + \delta], i')$ and $\sigma'((a', b'), j) = ([b', a' + \delta], j')$ with $\sigma^{\ker}([b, a + \delta], i') = ([b', a' + \delta], j')$. This implies $|b - b'| < 2\varepsilon$ and $|a - a'| = |(a + \delta) - (a' + \delta)| < 2\varepsilon$.
- If $((a', b'), j) \in \text{Rep } D(f')_o \setminus \text{im } \sigma^o$, then $\sigma((a', b'), j) = ([b', a' + \delta], j')$ and $\sigma^{\ker}([0, \delta], k) = ([b', a' + \delta], j')$, which implies that $a' = |(a' + \delta) - \delta| < 2\varepsilon$.

Therefore, the partial matching constructed fulfills all the requirements needed in the statement of Proposition Appendix B.2, concluding the proof. \square